Project Report on

CFD Modeling of Gas-Liquid-Solid Fluidized Bed

In partial fulfillment of the requirements of

Bachelor of Technology (Chemical Engineering)

Submitted By

Amit Kumar (Roll No.10500026)

Session: 2008-09

Under the guidance of

Mr. H.M. Jena

Department of Chemical Engineering

National Institute of Technology

Rourkela-769008

Orissa

CERTIFICATE

This is to certify that that the work in this thesis report entitled "**CFD Modeling of Gas-Liquid-Solid Fluidized Bed**" submitted by Amit Kumar in partial fulfillment of the requirements for the degree of Bachelor of Technology in Chemical Engineering Session 2005-2009 in the department of Chemical Engineering, National Institute of Technology Rourkela, Rourkela is an authentic work carried out by him under my supervision and guidance.

To the best of my knowledge the matter embodied in the thesis has not been submitted to any other University /Institute for the award of any degree.

Date:

Mr. H. M. Jena
Department of Chemical Engineering
National Institute of Technology
Rourkela - 769008

ACKNOWLEDGEMENT

With a feeling of great pleasure, I express my sincere gratitude to **Mr. H.M. Jena** for his superb guidance, support and constructive criticism, which led to the improvements and completion of this project work.

I am thankful to **Prof. R.K Singh** and **Prof. S.K. Maity** for acting as project coordinator.

I am also grateful to **Prof. K C Biswal**, Head of the Department, Chemical Engineering for providing the necessary opportunities for the completion of this project.

Amit Kumar (Roll No.10500026)

4^{th} year

B. Tech.

Department of Chemical Engineering

National Institute of Technology, Rourkela

ABSTRACT

Gas–liquid–solid fluidized beds are used extensively in the refining, petrochemical, pharmaceutical, biotechnology, food and environmental industries. Some of these processes use solids whose densities are only slightly higher than the density of water. Because of the good heat and mass transfer characteristics, three-phase fluidized beds or slurry bubble columns have gained considerable importance in their application in physical, chemical, petrochemical, electrochemical and biochemical processing.

This project report can be divided mainly into four parts. The first part discusses about importance of gas-liquid-solid fluidized bed, their modes of operation, important hydrodynamic properties those have been studied either related to modelling or experimental analysis and applications of gas-liquid-solid fluidized bed. The second part gives an overview of the methodology used in CFD to solve problems relating mass, momentum and heat transfer. Also comparative study of various CFD related software is given in this section. Third part contains the details about problem description and approach used in FLEUNT to get the solution. Finally results of simulation and comparison with experimental results are shown.

The experimental setup was a fluidized bed of height 1.88m and diameter 10cm. The gas (air) and liquid (water) is injected at the base with different velocities while taking glass beads of different diameters as solid bed. The variables to be investigated are pressure drop, gas holdup and bed expansion. It is required to verify the solutions of simulation by comparing it with experimental results and then rest of the prediction can be done instead of carrying out the experiments. In this way it helps to save the experimental costs and prevents from risk of wastage of resources.

CONTENTS

COVER PAGE		**i**
CERTIFICATE		**ii**
ACKNOWLEDGEMENT		**iii**
ABSTRACT		**iv**
CONTENTS		**v**
LIST OF TABLES AND FIGURES		**vii**
NOMENCLATURE		**ix**
CHAPTER 1	**LITERATURE REVIEW**	1
1.1	Introduction	1
1.2	Applications of Gas-liquid-solid fluidized bed	2
1.3	Modes of operation of Gas-liquid-solid fluidized bed and flow regimes	3
1.4	Important hydrodynamic parameters studied in gas-liquid-solid fluidization	6
1.5	Present work:	9
CHAPTER 2		11
2.1	CFD (Computational Fluid Dynamics)	11
2.1.1	Discretization Methods in CFD	11
2.1.1.1	Finite difference method (FDM)	11
2.1.1.2	Finite volume method (FVM)	11
2.1.1.3	Finite element method (FEM)	12
2.1.2	How does a CFD code work?	12
2.1.2.1	Pre-Processing	13
2.1.2.2	Solver	14
2.1.2.3	Post-Processing	17
2.1.3	Advantages of CFD	17
2.2	CFD modeling of multiphase systems:	18
2.2.1	Approaches for numerical calculations of multiphase flows	19
2.2.1.1	The Euler-Lagrange Approach:	19
2.2.1.2	The Euler-Euler Approach	19
2.2.1.2.1	The VOF Model:	20

2.2.1.2.2	The Mixture Model:	20
2.2.1.2.3	The Eulerian Model	20
2.2.2	Choosing a multiphase model	20
CHAPTER 3	**CFD SIMULATION OF GAS-LIQUID-SOLID FLUIDIZED BED**	22
3.1	Computational flow model	22
3.1.1	Equations	22
3.1.2	Turbulence modelling:	23
3.2	Problem description:	24
3.3	Simulation	25
3.3.1	Geometry and Mesh	25
3.3.2	Selection of models for simulation	26
3.3.3	Solution	27
CHAPTER 4	**RESULTS AND DISCUSSION**	28
4.1	Phase Dynamics	29
4.2	Bed Expansion	30
4.3	Gas Holdup	34
4.4.	Pressure Drop	36
CHAPTER 5	**CONCLUSION**	44
REFERENCES		45

.

LIST OF TABLES AND FIGURES

Table no.	Caption	Page no.
Table 1	Important hydrodynamic parameters studied by CFD modeling of solid-liquid-gas fluidized bed.	8
Table 2	**P**roperties of air, water and glass beads used in experiment	24
Table 3	Model constants used for simulation	26
Figure no.		
Figure 1	Taxonomy of Three-Phase Fluidized Beds	4
Figure 2	Modes of operation of gas-liquid-solid fluidized bed	4
Figure 3	Schematic representation of the Mode I-a fluidized bed reactor	6
Figure 4	Algorithm of numerical approach used by simulation softwares	16
Figure 5	Experimental setup of fluidized bed column used (Static bed heights=17.1cm, 21.3cm)	24
Figure 6	Coarse mesh and fine mesh created in GAMBIT	25
Figure 7	Plot of residuals for k-epsilon solver method as the iterations proceeds.	27
Figure 8	Contours of volume fraction of glass beads at water velocity of 0.12m/s and air velocity of 0.0125m/s with respect of time for initial bed height 21.3cm.	28
Figure 9	Contours of volume fractions of solid, liquid and gas at water velocity of 0.12m/s and air velocity of 0.0125m/s for initial bed height 21.3cm.	29
Figure 10	Velocity vector of glass beads in the column (actual and magnified)	30
Figure 11	Velocity vector of water in the column (actual and magnified**)**	31
Figure 12	Velocity vector of air in the column (actual and magnified)	32
Figure 13	XY plot of velocity magnitude of water	33
Figure 14	XY plot of velocity magnitude of air	33
Figure 15	Contours of volume fraction of glass beads with increasing water velocity at inlet air velocity 0.05m/s for initial bed height 17.1cm and glass beads of size 2.18mm	34
Figure 16	XY plot of volume fraction of glass beads	35
Figure 17	Bed expansion vs. water velocity for initial bed height 17.1 cm and particle size 2.18mm	36

Figure 18	Bed expansion vs. water Velocity for initial bed height 21.3 cm and particle size 2.18mm	36
Figure 19	Comparison of experimental results and simulated results obtained at air velocity 0.05m/s and initial bed height 17.1 cm	37
Figure 20	Contour of air volume fraction at water velocity of 0.12m/s and air velocity of 0.0125m/s for initial bed height 21.3cm	38
Figure 21	Gas holdup vs. water velocity for initial bed height 17.1 cm and particle size 2.18mm	38
Figure 22	Gas holdup vs. water velocity for initial bed height 21.3 cm and particle size 2.18mm	39
Figure 23	Gas holdup vs. water velocity for initial bed height 17.1 cm and particle size 2.18mm	39
Figure 24	Gas holdup vs. air velocity for initial bed height 21.3 cm and particle size 2.18mm	40
Figure 25	Comparison of experimental result of gas holdup with that of simulated result obtained at air inlet velocities 0.025 m/s and 0.05m/s for initial bed height 21.3 cm	40
Figure 26	Contours of static gauge pressure (mixture phase) in the column obtained at water velocity of 0.12m/s and air velocity of 0.0125m/s.	41
Figure 27	Pressure Drop vs. water velocity for initial bed height 17.1 cm and particle size 2.18mm	42
Figure 28	Pressure Drop vs. water velocity for initial bed height 21.3 cm and particle size 2.18 mm	42
Figure 29	Pressure Drop vs. Air velocity for initial bed height 17.1 cm and particle size 2.18mm	43
Figure 30	Pressure Drop vs. Air velocity for initial bed height 21.3 cm and particle size 2.18mm	43
Figure 31	Comparison between pressure drop from experiment and that from simulation at air inlet velocity 0.025 m/s and 0.025 m/s for initial bed height 21.3 cm	44

Nomenclature

ρ_k = Density of phase k= g (gas), l (liquid), s (solid)

ε_k= Volume fraction of phase k= g (gas), l (liquid), s (solid)

$\vec{u}_k$= Velocity of phase k= g (gas), l (liquid), s (solid)

P= Pressure

μ_{eff}= Effective viscosity

$M_{i,l}$= interphase force term for liquid phase

$M_{i,g}$= interphase force term for gas phase

$M_{i,s}$= interphase force term for solid phase

K= Turbulent kinetic energy

ε= Dissipation rate of turbulent kinetic energy

t= Time

g= Acceleration due to gravity

CHAPTER 1
LITERATURE REVIEW

1.1. INTRODUCTION

In a typical gas–liquid–solid three-phase fluidized bed, solid particles are fluidized primarily by upward concurrent flow of liquid and gas, with liquid as the continuous phase and gas as dispersed bubbles if the superficial gas velocity is low. Because of the good heat and mass transfer characteristics, three-phase fluidized beds or slurry bubble columns ($u_t < 0.05$ m/s) have gained considerable importance in their application in physical, chemical, petrochemical, electrochemical and biochemical processing (L. S. Fan, 1989).

Gas–liquid–solid fluidized beds are used extensively in the refining, petrochemical, pharmaceutical, biotechnology, food and environmental industries. Some of these processes use solids whose densities are only slightly higher than the density of water (Bigot et al., 1990; Fan, 1989; Merchant; Nore, 1992).

Gas–liquid–solid fluidized beds can be operated with different hydrodynamic regimes, which depend on the gas and liquid velocities, as well as the gas, liquid and solid properties. For proper reactor modelling, it is essential to know under which regime the reactor will be operating (Briens et al., 2005).

Two important hydrodynamic transitions within gas– liquid–solid fluidized beds are the minimum liquid fluidization velocity, U_{Lmf}, and the transition velocity from the coalesced to dispersed bubble regime, U_{cd}. The minimum liquid fluidization velocity is the superficial liquid velocity at which the bed becomes fluidized for a given superficial gas velocity; above the minimum liquid fluidization velocity, there is good contact between the gas, liquid and solid phases which is essential for heat and mass transfer processes. In the coalesced bubble regime, bubble size varies as the bubbles continuously coalesce and split, while in the dispersed bubble regime, there is no coalescence and thus the bubble size is more uniform and generally smaller (Luo et al., 1997).

Intensive investigations have been performed on three-phase fluidization over the past few decades; however, there is still a lack of detailed physical understanding and predictive tools for proper design, scale-up and optimum operation of such reactors. The calculation of hydrodynamic parameters in these systems mainly relies on empirical correlations or semi-

theoretical models such as the generalized wake model (Epstein et al., 1974) and the structured wake model (L. S. Fan, 1989).

Though these models are capable of successfully elucidating the phenomena occurring in the three-phase reactors, too many parameters in them have limited their practical applications. In recent years, the computational fluid dynamics (CFD) based on the fundamental conservation equations has become a viable technique for process simulation. Although powerful computer capability is available today, CFD is very expensive in terms of computer resources and time for full-scale, high-resolution, two- or three-dimensional simulation, and it is not readily applicable for routine design and scale-up of industrial-scale units, at least at present. Hence, there is a practical need to develop general and simple models for the three-phase fluidized beds. FLUENT and CFX are tools normally used to get CFD solutions of three phase fluidized bed.

1.2. Applications of Gas-liquid-solid fluidized bed

Gas-liquid-solid fluidized beds have emerged in recent years as one of the most promising devices for three-phase operations. Such devices are of considerable industrial importance as evidenced by their wide use for chemical, petrochemical and biochemical processing. As three-phase reactors, they have been employed in hydrogenation and hydrosulferization of residual oil for coal liquefaction, in turbulent contacting absorption for flue gas desulphurization, and in the bio-oxidation process for wastewater treatment. Three-phase fluidized beds are also often used in physical operations.

The application of gas-liquid-solid fluidized bed systems to biotechnological processes such as fermentation and aerobic wastewater treatment has gained considerable attention in recent years. In these three-phase biotechnological processes, biologically catalytic agents, either enzymes or living cells, are incorporated into the solid phase through immobilization techniques. Typically, enzymes or living cells are entrapped within natural or synthetic polymer gel particles or are attached to the surface of solid particles. Three-phase fluidized beds enjoy widespread use in a number of applications including hydro treating and conversion of heavy petroleum and synthetic crude, coal liquefaction, methanol production, conversion of glucose to ethanol and various hydrogenation and oxidation reaction.

Fluidized bed units are also found in many plant operations in pharmaceuticals and mineral industries. Fluidized beds serve many purposes in industry, such as facilitating catalytic and non-

catalytic reactions, drying and other forms of mass transfer. They are especially useful in the fuel and petroleum industry for things such as hydrocarbon cracking and reforming as well as oxidation of naphthalene to phathalic anhydride (catalytic), or coking of petroleum residues (non-catalytic). Catalytic reactions are carried out in fluidized beds by using a catalyst as the cake in the column, and then introducing the reactants. In catalytic reactions, gas or liquid is passed through a dry catalyst to speed up the reaction.

1.3. Modes of operation of Gas-liquid-solid fluidized bed and flow regimes

Gas-liquid-solid fluidization can be classified mainly into four modes of operation. These modes are co-current three-phase fluidization with liquid as the continuous phase (mode I-a); co-current three-phase fluidization with gas as the continuous phase (mode-I-b); inverse three-phase fluidization (mode II-a); and fluidization represented by a turbulent contact absorber (TCA) (mode II-b). Modes II-a and II-b are achieved with a countercurrent flow of gas and liquid. Due to the complex nature of three-phase fluidization, however, various method are possible in evaluating the operating and design parameters for each mode of operation.

Based on the differences in flow directions of gas and liquid and in contacting patterns between the particles and the surrounding gas and liquid, several types of operation for gas-liquid-solid fluidizations are possible. Three-phase fluidization is divided into two types according to the relative direction of the gas and liquid flows, namely, co-current three-phase fluidization and co-current three-phase fluidization (Bhatia and Epstein, 1974b; Epstein, 1981). This is shown in **Fig. 1.**

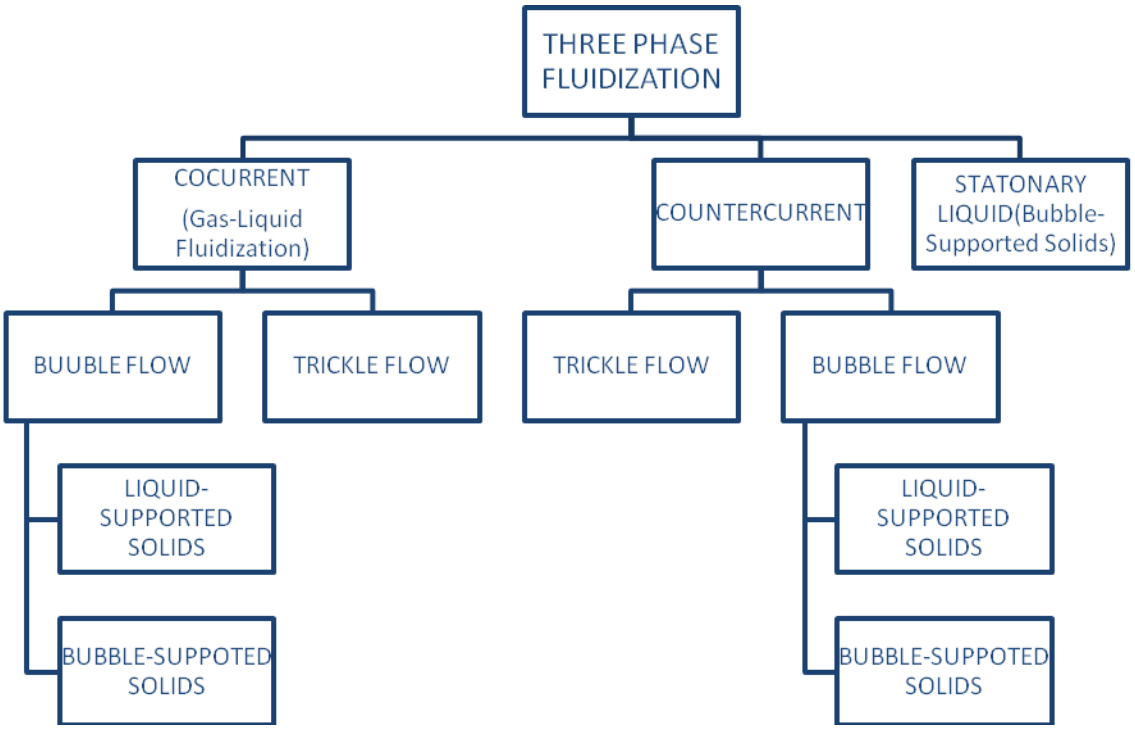

Fig.1. Taxonomy of Three-Phase Fluidized Beds (Epstein, 1981)

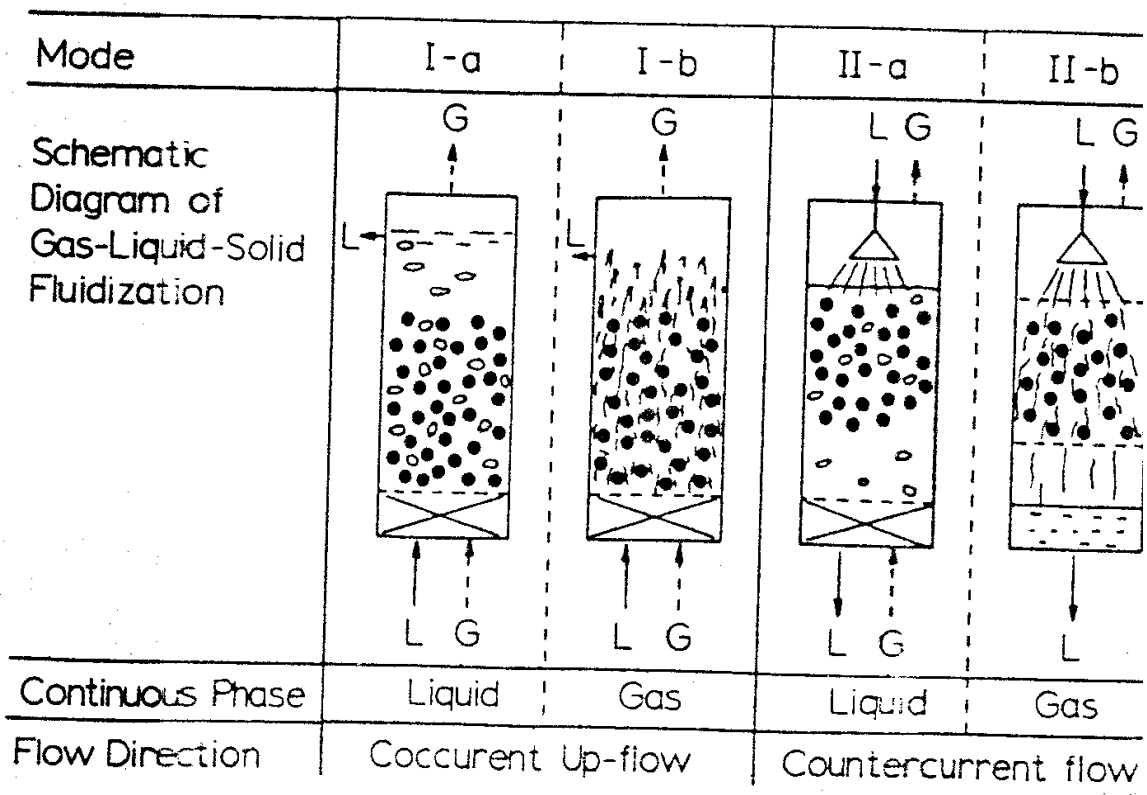

Fig.2. Modes of operation of gas-liquid-solid fluidized bed

In co-current three-phase fluidization, there are two contacting modes characterized different hydrodynamic conditions between the solid particles and the surrounding gas and liquid. These modes are denoted as mode I-a and mode I–b**,** (Fig. 2). Mode I-a defines co-current three-phase fluidization with liquid as the continuous phase, while mode I-b defines co-current three-phase fluidization with gas as the continuous phase. In mode I-a fluidization, the liquid with the gas-forming discrete bubbles supports the particles. Mode I-a is generally referred as to as gas-liquid fluidization. The term bubble flow, in Epstein's taxonomy (1981), includes two types of flow for mode I-a; namely, liquid-supported solids and bubble supported solids.

According to Epstein (1981, 1983), the liquid-supported solids operation characterizes fluidization with the liquid velocity beyond the minimum fluidization velocity; the bubble-supported solids operation characterizes fluidization with the liquid velocity below the minimum fluidization velocity where the liquid may even be in a stationary state. Countercurrent three-phase fluidization with liquid as the continuous phase, denoted as mode II-a in figure-2, is known as inverse three-phase fluidization. Countercurrent three-phase fluidization with gas as the continuous phase, denoted as mode II-b in figure-2, is known as a turbulent contact absorber, fluidized packing absorber, mobile bed, or turbulent bed contactor. In mode II-a operation the bed of particles with density lower than that of the liquid is fluidized by a downward liquid flow, opposite to the net buoyant force on the particles, while the gas is introduced counter currently to that liquid forming discrete bubbles in the bed. In the mode II-b operation (TCA operation), an irrigated bed of low-density particles is fluidized by the upward flow of gas as a continuous phase. When the bed is in a fully fluidized state, the vigorous moment of wetted particles give rise to excellent gas-liquid contacting. The gas and liquid flow rates in the TCA are much higher than those possible in conventional countercurrent packed beds, since the bed can easily exposed to reduce hydrodynamics resistances.

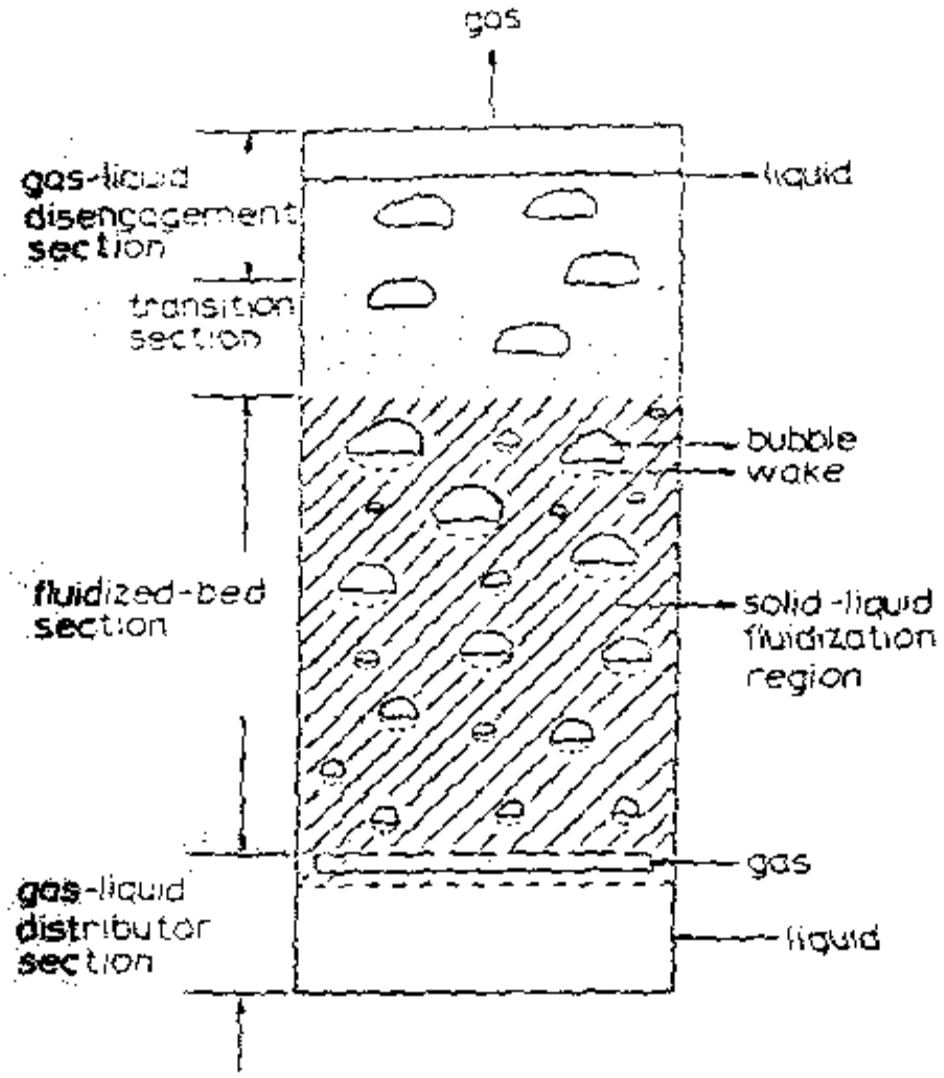

Fig.3. Schematic representation of the Mode I-a fluidized bed reactor

1.4. Important hydrodynamic parameters studied in gas-liquid-solid fluidization

Most of the previous studies related to three-phase fluidized bed reactors have been directed towards the understanding the complex hydrodynamics, and its influence on the phase holdup and transport properties. In literature, the hydrodynamic behavior, viz., the pressure drop, minimum fluidization velocity, bed expansion and phase hold-up of a co-current gas–liquid–solid three-phase fluidized bed, were examined using liquid as the continuous phase and gas as the discontinuous phase (Jena et al. 2008). Recent research on fluidized bed reactors focuses on the following topics:

(a) Flow structure quantification: The quantification of flow structure in three-phase fluidized beds mainly focuses on local and globally averaged phase holdups and phase velocities for different operating conditions and parameters. Rigby et al.(1970), Muroyama and Fan(1985), Lee and DeLasa(1987), Yu and Kim(1988) investigated bubble phase holdup and velocity in three-phase fluidized beds for various operating conditions using experimental techniques like electro-resistivity probe and optical fiber probe. Larachi et al. (1996), Kiared et al. (1999) investigated the solid phase hydrodynamics in three-phase fluidized bed using radio active particle tracking. Recently Warsito and Fan (2001, 2003) quantified the solid and gas holdup in three-phase fluidized bed using the electron capacitance tomography (ECT).

(b) Flow regime identification: Muroyama and Fan (1985) developed the flow regime diagram for air–water–particle fluidized bed for a range of gas and liquid superficial velocities. Chen et al. (1995) investigated the identification of flow regimes by using pressure fluctuations measurements. Briens and Ellis(2005) used spectral analysis of the pressure fluctuation for identifying the flow regime transition from dispersed to coalesced bubbling flow regime based on various data mining methods like fractal and chaos analysis, discrete wake decomposition method etc. Fraguío et al.(2006) used solid phase tracer experiments for flow regime identification in three phase fluidized beds.

(c) Advanced modeling approaches: Even though a large number of experimental studies have been directed towards the quantification of flow structure and flow regime identification for different process parameters and physical properties, the complex hydrodynamics of these reactors are not well understood due to complicated phenomena such as particle–particle, liquid–particle and particle–bubble interactions. For this reason, computational fluid dynamics (CFD) has been promoted as a useful tool for understanding multiphase reactors (Dudukovic etal., 1999) for precise design and scale up. Basically two approaches are used namely, the Euler–Euler formulation based on the interpenetrating multi-fluid model, and the Euler–Lagrangian approach based on solving Newton's equation of motion for the dispersed phase. Recently, several CFD models based on Eulerian multi-fluid approach have been developed for gas–liquid flows (Kulkarni et al., 2007; Cheungetal. 2007) and liquid–solid flows(Roy and Dudukovic, 2001; Panneerselvam etal.,2007) and gas–solid flows (Jiradilok etal.,2007). Some of the authors

(Matonis et al., 2002; Feng et al., 2005; Schallenberg et al.,2005) have extended these models to three-phase flow systems.

Comprehensive list of literature on modeling of these reactors are tabulated in Table 1. Most of these CFD studies are based on steady state, 2-D axis-symmetric, Eulerian multi-fluid approach. But in general, three phase flows in fluidized bed reactors are intrinsically unsteady and are composed of several flow processes occurring at different time and length scales. The unsteady fluid dynamics often govern the mixing and transport processes and is inter-related in a complex way with the design and operating parameters like reactor and sparger configuration, gas flow rate and solid loading.

Table1. Important hydrodynamic parameters studied by CFD modeling of solid-liquid-gas fluidized bed.

Authors	Multiphase approach	Models used	Parameter studied
Bahary et al. (1994)	Multi fluid Eulerian approach for three phase fluidized bed	Gas phase was treated as a particulate phase having 4mm diameter and a kinetic theory granular flow model applied for solid phase. They have simulated both sym metric and axis-symmetric mode	Verified the different flow regimes in the fluidized bed and compared the time averaged axial solid velocity with experimental data
Grevskott et al. (1996)	Two fluid Eulerian–Eulerian model for three phase bubble column	The liquid phase along with the particles is considered pseudo homogeneous by modifying the viscosity and density. They included the bubble size distribution based on the bubble induced turbulent length scale and the local turbulent kinetic energy level	Studied the variation of bubble size distribution, liquid circulation and solid movement
Mitra-Majumdar et al.(1997)	2-D axis-symmetric, multi-fluid Eulerian approach for three-phase bubble column	Used modified drag correlation between the liquid and the gas phase to account for the effect of solid particles and between the solid of gas bubbles. A k– ε turbulence model was used for the turbulence and considered the effect of bubbles on liquid phase turbulence	Examined axial variation of gas holdup and solid hold up profiles for various range of liquid and gas superficial velocities and solid circulation velocity
Jianping and Shonglin(1998)	2-D, Eulerian–Eulerian method for three-phase bubble column	Pseudo-two-phase fluid dynamic model. k_{sus}– ε $_{sus}$–k_b– ε_b turbulence model used for turbulence	Validated local axial liquid velocity and local gas holdup with experimental data
Padial et al. (2000)	3-D, multi-fluid Eulerian approach for three-phase draft- tube bubble column	The drag force between solid particles and gas bubbles was modeled in the same way as that of drag force between liquid and gas bubbles	Simulated gas volume fraction and liquid circulation in draft tube bubble column. contd…
Matonis et al.(2002)	3-D, multi-fluid Eulerian approach for	Kinetic theory granular flow(KTGF)model for describing the	Studied the time averaged solid velocity and volume

	slurry bubble column	particulate phase and a k– ε based turbulence model for liquid phase turbulence	fraction profiles, normal and shear Reynolds stress and comparison with experimental data
Feng et al.(2005)	3-D, multi-fluid Eulerian approach for three-phase bubble column	The liquid phase along with the solid phase considered as a pseudo homogeneous phase in view of the ultrafine nanoparticles. The interface force model of drag, lift and virtual mass and k– ε model for turbulence are included	Compared the local time averaged liquid velocity and gas holdup profiles along the radial position
Schallenberg et al.(2005)	3-D, multi-fluid Eulerian approach for three-phase bubble column	Gas–liquid drag coefficient based on single bubble rise, which is modified for the effect of solid phase. Extended k– ε turbulence model to account for bubble-induced turbulence. The interphase momentum between two dispersed phases is included.	Validated local gas and solid holdup as well as liquid velocities with experimental data
Li et al. (1999)	2-D, Eulerian–Lagrangian model for three-phase fluidization	The Eulerian fluid dynamic (CFD) method, the dispersed particle method (DPM) and the volume-of-fluid (VOF) method are used to account for the flow of liquid, solid, and gas phases, respectively. A continuum surface force (CSF) model, a surface tension force model and Newton's third law are applied to account for the interphase couplings of gas–liquid, particle–bubble and particle–liquid interactions, respectively. A close distance interaction (CDI) model is included in the particle–particle collision analysis, which considers the liquid interstitial effects between colliding particles	Investigated single bubble rising velocity in a liquid–solid fluidized bed and the bubble wake structure and bubble rise velocity in liquid and liquid–solid medium are simulated
Zhang and Ahmadi (2005)	2-D, Eulerian–Lagrangian model for three-phase slurry reactor	The interactions between bubble–liquid and particle–liquid are included. The drag, lift, buoyancy, and virtual mass forces are also included. Particle–particle and bubble–bubble interactions are accounted for by the hard sphere model approach. Bubble coalescence is also included in the model	Studied transient characteristics of gas, liquid, and particle phase flows in terms of flow structure and instantaneous velocities. The effect of bubble size on variation of flow patterns are also studied

1.5. Present work:

In the studies done so far, there has not been much emphasis on gas holdup and pressure drop. Here, the focus is on understanding the complex hydrodynamics of three-phase fluidized beds containing coarser particles of size above 1mm. The CFD software package FLUENT 6.2.16 has been used to simulate a solid-liquid-gas fluidized bed with a special designed air

sparger aimed at improving the gas-liquid mixing in the distributor section and sending the well mixed gas-liquid mixture to the fluidizing section. The fluidized bed to be simulated is of height 1.88m and diameter 0.1m. The gas (air) and liquid (water) has been injected at the base with different velocities while taking glass beads of diameter 2.18mm as solid bed. The variables to be investigated are bed expansion, gas holdup and pressure drop. The static bed heights of the solid phase in the fluidized bed used for simulation are 17.1 cm and 21.3 cm. The simulated results have been compared with the experimental results of Jena et al. (2008).

Definitions

Bed expansion: The height in the column up to which the solid phase is found in fluidized condition.

Gas holdup: Gas holdup is defined as volume fraction of gas phase in that the column. In contrast to gas-solid-liquid fluidized bed gas holdup is taken for expanded part of the column.

Pressure drop: Pressure drop is defined as the difference of absolute pressure of inlet to that of the outlet.

CHAPTER 2
CFD IN MULTIPHASE MODELING

2.1. CFD (Computational Fluid Dynamics)

CFD is one of the branches of fluid mechanics that uses numerical methods and algorithms to solve and analyze problems that involve fluid flows. Computers are used to perform the millions of calculations required to simulate the interaction of fluids and gases with the complex surfaces used in engineering. However, even with simplified equations and high speed supercomputers, only approximate solutions can be achieved in many cases. More accurate codes that can accurately and quickly simulate even complex scenarios such as supersonic or turbulent flows are an ongoing area of research.

2.1.1. Discretization Methods in CFD

There are three discretization methods in CFD:

1. Finite difference method (FDM)
2. Finite volume method (FVM)
3. Finite element method (FEM)

2.1.1.1. Finite difference method (FDM): A finite difference method (FDM) discretization is based upon the differential form of the PDE to be solved. Each derivative is replaced with an approximate difference formula (that can generally be derived from a Taylor series expansion). The computational domain is usually divided into hexahedral cells (the grid), and the solution will be obtained at each nodal point. The FDM is easiest to understand when the physical grid is Cartesian, but through the use of curvilinear transforms the method can be extended to domains that are not easily represented by brick-shaped elements. The discretization results in a system of equation of the variable at nodal points, and once a solution is found, then we have a discrete representation of the solution.

2.1.1.2. Finite volume method (FVM): A finite volume method (FVM) discretization is based upon an integral form of the PDE to be solved (e.g. conservation of mass, momentum, or energy). The PDE is written in a form which can be solved for a given finite volume (or cell). The computational domain is discretized into finite volumes and then for every volume the

governing equations are solved. The resulting system of equations usually involves fluxes of the conserved variable, and thus the calculation of fluxes is very important in FVM. The basic advantage of this method over FDM is it does not require the use of structured grids, and the effort to convert the given mesh in to structured numerical grid internally is completely avoided. As with FDM, the resulting approximate solution is a discrete, but the variables are typically placed at cell centers rather than at nodal points. This is not always true, as there are also face-centered finite volume methods. In any case, the values of field variables at non-storage locations (e.g. vertices) are obtained using interpolation.

2.1.1.3. Finite element method (FEM): A finite element method (FEM) discretization is based upon a piecewise representation of the solution in terms of specified basis functions. The computational domain is divided up into smaller domains (finite elements) and the solution in each element is constructed from the basis functions. The actual equations that are solved are typically obtained by restating the conservation equation in weak form: the field variables are written in terms of the basis functions, the equation is multiplied by appropriate test functions, and then integrated over an element. Since the FEM solution is in terms of specific basis functions, a great deal more is known about the solution than for either FDM or FVM. This can be a double-edged sword, as the choice of basis functions is very important and boundary conditions may be more difficult to formulate. Again, a system of equations is obtained (usually for nodal values) that must be solved to obtain a solution.

Comparison of the three methods is difficult, primarily due to the many variations of all three methods. FVM and FDM provide discrete solutions, while FEM provides a continuous (up to a point) solution. FVM and FDM are generally considered easier to program than FEM, but opinions vary on this point. FVM are generally expected to provide better conservation properties, but opinions vary on this point also.

2.1.2. How does a CFD code work?

CFD codes are structured around the numerical algorithms that can be tackle fluid problems. In order to provide easy access to their solving power all commercial CFD packages include sophisticated user interfaces input problem parameters and to examine the results. Hence all codes contain three main elements:

1. Pre-processing.
2. Solver
3. Post-processing.

2.1.2.1. Pre-Processing:

This is the first step in building and analyzing a flow model. Preprocessor consist of input of a flow problem by means of an operator –friendly interface and subsequent transformation of this input into form of suitable for the use by the solver. The user activities at the Pre-processing stage involve:

- Definition of the geometry of the region: The computational domain.
- Grid generation the subdivision of the domain into a number of smaller, non-overlapping sub domains (or control volumes or elements Selection of physical or chemical phenomena that need to be modeled).
- Definition of fluid properties
- Specification of appropriate boundary conditions at cells, which coincide with or touch the boundary. The solution of a flow problem (velocity, pressure, temperature etc.) is defined at nodes inside each cell. The accuracy of CFD solutions is governed by number of cells in the grid. In general, the larger numbers of cells better the solution accuracy. Both the accuracy of the solution & its cost in terms of necessary computer hardware & calculation time are dependent on the fineness of the grid. Efforts are underway to develop CFD codes with a (self) adaptive meshing capability. Ultimately such programs will automatically refine the grid in areas of rapid variation.

GAMBIT (CFD PREPROCESSOR): GAMBIT is a state-of-the-art preprocessor for engineering analysis. With advanced geometry and meshing tools in a powerful, flexible, tightly-integrated, and easy-to use interface, GAMBIT can dramatically reduce preprocessing times for many applications. Complex models can be built directly within GAMBIT's solid geometry modeler, or imported from any major CAD/CAE system. Using a virtual geometry overlay and advanced cleanup tools, imported geometries are quickly converted into suitable flow domains. A comprehensive set of highly-automated and size function driven meshing tools ensures that the best mesh can be generated, whether structured, multiblock, unstructured, or hybrid.

2.1.2.2. Solver:

The CFD solver does the flow calculations and produces the results. FLUENT, FloWizard, FIDAP, CFX and POLYFLOW are some of the types of solvers. FLUENT is used in most industries. FloWizard is the first general-purpose rapid flow modeling tool for design and process engineers built by Fluent. POLYFLOW (and FIDAP) are also used in a wide range of fields, with emphasis on the materials processing industries. FLUENT and CFX two solvers were developed independently by ANSYS and have a number of things in common, but they also have some significant differences. Both are control-volume based for high accuracy and rely heavily on a pressure-based solution technique for broad applicability. They differ mainly in the way they integrate the fluid flow equations and in their equation solution strategies. The CFX solver uses finite elements (cell vertex numerics), similar to those used in mechanical analysis, to discretize the domain. In contrast, the FLUENT solver uses finite volumes (cell centered numerics). CFX software focuses on one approach to solve the governing equations of motion (coupled algebraic multigrid), while the FLUENT product offers several solution approaches (density-, segregated- and coupled-pressure-based methods)

The FLUENT CFD code has extensive interactivity, so we can make changes to the analysis at any time during the process. This saves time and enables to refine designs more efficiently. Graphical user interface (GUI) is intuitive, which helps to shorten the learning curve and make the modeling process faster. In addition, FLUENT's adaptive and dynamic mesh capability is unique and works with a wide range of physical models. This capability makes it possible and simple to model complex moving objects in relation to flow. This solver provides the broadest range of rigorous physical models that have been validated against industrial scale applications, so we can accurately simulate real-world conditions, including multiphase flows, reacting flows, rotating equipment, moving and deforming objects, turbulence, radiation, acoustics and dynamic meshing. The FLUENT solver has repeatedly proven to be fast and reliable for a wide range of CFD applications. The speed to solution is faster because suite of software enables us to stay within one interface from geometry building through the solution process, to post-processing and final output.

The numerical solution of Navier–Stokes equations in CFD codes usually implies a discretization method: it means that derivatives in partial differential equations are approximated by algebraic expressions which can be alternatively obtained by means of the finite-difference or the finite-element method. Otherwise, in a way that is completely different from the previous one, the discretization equations can be derived from the integral form of the conservation equations: this approach, known as the finite volume method, is implemented in FLUENT (FLUENT user's guide, vols. 1–5, Lebanon, 2001), because of its adaptability to a wide variety of grid structures. The result is a set of algebraic equations through which mass, momentum, and energy transport are predicted at discrete points in the domain. In the freeboard model that is being described, the segregated solver has been chosen so the governing equations are solved sequentially. Because the governing equations are non-linear and coupled, several iterations of the solution loop must be performed before a converged solution is obtained and each of the iteration is carried out as follows:

(1) Fluid properties are updated in relation to the current solution; if the calculation is at the first iteration, the fluid properties are updated consistent with the initialized solution.

(2) The three momentum equations are solved consecutively using the current value for pressure so as to update the velocity field.

(3) Since the velocities obtained in the previous step may not satisfy the continuity equation, one more equation for the pressure correction is derived from the continuity equation and the linearized momentum equations: once solved, it gives the correct pressure so that continuity is satisfied. The pressure–velocity coupling is made by the SIMPLE algorithm, as in FLUENT default options.

(4) Other equations for scalar quantities such as turbulence, chemical species and radiation are solved using the previously updated value of the other variables; when inter-phase coupling is to be considered, the source terms in the appropriate continuous phase equations have to be updated with a discrete phase trajectory calculation.

(5) Finally, the convergence of the equations set is checked and all the procedure is repeated until convergence criteria are met. (Ravelli et al., 2008)

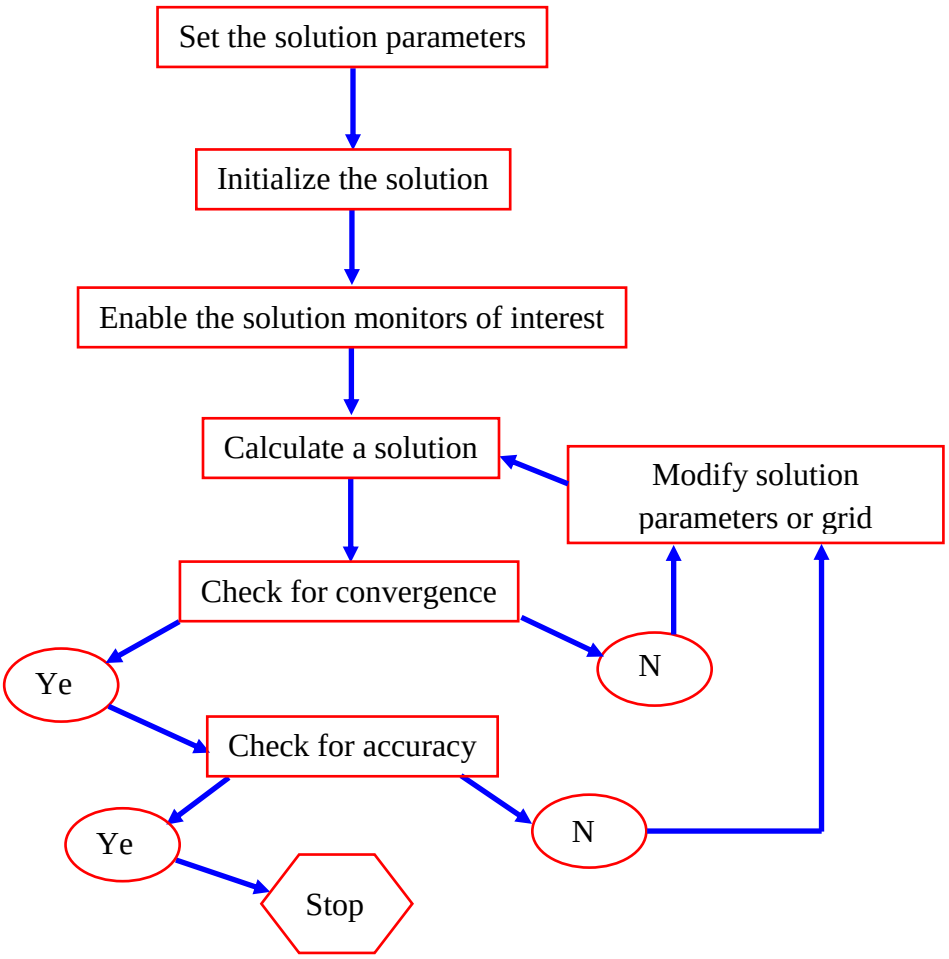

Fig.4. Algorithm of numerical approach used by simulation softwares

The conservation equations are linearized according to the implicit scheme with respect to the dependent variable: the result is a system of linear equations (with one equation for each cell in the domain) that can be solved simultaneously. Briefly, the segregated implicit method calculates every single variable field considering all the cells at the same time. The code stores discrete values of each scalar quantity at the cell centre; the face values must be interpolated from the cell centre values. For all the scalar quantities, the interpolation is carried out by the second order upwind scheme with the purpose of achieving high order accuracy. The only exception is represented by pressure interpolation, for which the standard method has been chosen. Ravelli et al., 2008).

2.1.2.3 Post-Processing:

This is the final step in CFD analysis, and it involves the organization and interpretation of the predicted flow data and the production of CFD images and animations. Fluent's software includes full post processing capabilities. FLUENT exports CFD's data to third-party post-processors and visualization tools such as Ensight, Fieldview and TechPlot as well as to VRML formats. In addition, FLUENT CFD solutions are easily coupled with structural codes such as ABAQUS, MSC and ANSYS, as well as to other engineering process simulation tools.

Thus FLUENT is general-purpose computational fluid dynamics (CFD) software ideally suited for incompressible and mildly compressible flows. Utilizing a pressure-based segregated finite-volume method solver, FLUENT contains physical models for a wide range of applications including turbulent flows, heat transfer, reacting flows, chemical mixing, combustion, and multiphase flows. FLUENT provides physical models on unstructured meshes, bringing you the benefits of easier problem setup and greater accuracy using solution-adaptation of the mesh. FLUENT is a computational fluid dynamics (CFD) software package to simulate fluid flow problems. It uses the finite-volume method to solve the governing equations for a fluid. It provides the capability to use different physical models such as incompressible or compressible, inviscid or viscous, laminar or turbulent, etc. Geometry and grid generation is done using GAMBIT which is the preprocessor bundled with FLUENT. Owing to increased popularity of engineering work stations, many of which has outstanding graphics capabilities, the leading CFD are now equipped with versatile data visualization tools. These include

- Domain geometry & Grid display.
- Vector plots.
- Line & shaded contour plots.
- 2D & 3D surface plots.
- Particle tracking.
- View manipulation (translation, rotation, scaling etc.)

2.1.3. Advantages of CFD:

Major advancements in the area of gas-solid multiphase flow modeling offer substantial process improvements that have the potential to significantly improve process plant operations. Prediction of gas solid flow fields, in processes such as pneumatic transport lines, risers,

fluidized bed reactors, hoppers and precipitators are crucial to the operation of most process plants. Up to now, the inability to accurately model these interactions has limited the role that simulation could play in improving operations. In recent years, computational fluid dynamics (CFD) software developers have focused on this area to develop new modeling methods that can simulate gas-liquid-solid flows to a much higher level of reliability. As a result, process industry engineers are beginning to utilize these methods to make major improvements by evaluating alternatives that would be, if not impossible, too expensive or time-consuming to trial on the plant floor. Over the past few decades, CFD has been used to improve process design by allowing engineers to simulate the performance of alternative configurations, eliminating guesswork that would normally be used to establish equipment geometry and process conditions. The use of CFD enables engineers to obtain solutions for problems with complex geometry and boundary conditions. A CFD analysis yields values for pressure, fluid velocity, temperature, and species or phase concentration on a computational grid throughout the solution domain. Advantages of CFD can be summarized as:

1. It provides the flexibility to change design parameters without the expense of hardware changes. It therefore costs less than laboratory or field experiments, allowing engineers to try more alternative designs than would be feasible otherwise.

2. It has a faster turnaround time than experiments.

3. It guides the engineer to the root of problems, and is therefore well suited for trouble-shooting.

4. It provides comprehensive information about a flow field, especially in regions where measurements are either difficult or impossible to obtain.

2.2. CFD modeling of multiphase systems

This section focuses on CFD modeling of multiphase systems. Following are some examples of multiphase systems:

- Bubbly flow examples: absorbers, aeration, airlift pumps, cavitations, evaporators, flotation and scrubbers.
- Droplet flow examples: absorbers, atomizers, combustors, cryogenic pumping, dryers, evaporation, gas cooling and scrubbers.
- Slug flow examples: large bubble motion in pipes or tanks.

2.2.1. Approaches for numerical calculations of multiphase flows

In the case of multiphase flows currently there are two approaches for the numerical calculations:

1. Euler-Lagrange approach
2. Euler-Euler approach

2.2.1.1. The Euler-Lagrange Approach:

The Lagrangian discrete phase model follows the Euler-Lagrange approach. The fluid phase is treated as a continuum by solving the time-averaged Navier- Stokes equations, while the dispersed phase is solved by tracking a large number of particles, bubbles, or droplets through the calculated flow field. The dispersed phase can exchange momentum, mass and energy with the fluid phase. A fundamental assumption made in this model is that the dispersed second phase occupies a low volume fraction, even though high mass loading, $m_{particle} >= m_{fluid}$ is acceptable. The particle or droplet trajectories are computed individually at specified intervals during the fluid phase calculation. This makes the model appropriate for the modeling of spray dryers, coal and liquid fuel combustion, and some particle laden flows, but inappropriate for the modeling of liquid-liquid mixtures, fluidized beds or any application where the volume fraction of the second phase is not negligible.

2.2.1.2. The Euler-Euler Approach

In the Euler-Euler approach the different phases are treated mathematically as interpenetrating continua. Since the volume of a phase can not be carried occupied by the other phases, the concept of the volume fraction is introduced. These volume fractions are assumed to be continuous functions of space and time and their sum is equal to one. Conservation equations for each phase are derived to obtain a set of equations, which have similar structure for all phases. These equations are closed by providing constitutive relations that are obtained from empirical information or in the case of granular flows by application of kinetic theory. There are three different Euler-Euler multiphase models available: The volume of fluid (VOF) model, the mixture model and The Eulerian model.

2.2.1.2.1. The VOF Model:

The VOF model is a surface tracking technique applied to a fixed Eulerian mesh. It is designed for two or more immiscible fluids where the position of the interface between the fluids is of interest. In the VOF model, a single set of momentum equations is shared by the fluids and the volume fraction of each of the fluids in each computational cell is tracked throughout the domain. The applications of VOF model include stratified flows, free surface flows, filling, sloshing, and the motion of large bubbles in a liquid, the motion of liquid after a dam break, the prediction of jet breakup (surface tension) and the steady or transient tracking of any liquid- gas interface.

2.2.1.2.2. The Mixture Model:

The mixture model is designed for two of more phases (fluid or particulate). As in the Eulerian model, the phases are treated as interpenetrating continua. The mixture model solves for the mixture momentum equation and prescribes relative velocities to describe the dispersed phase. Applications of the mixture model include particle-laden flows with low loading, bubbly flows, and sedimentation and cyclone separators. The mixture model can also be used without relative velocities for the dispersed phase to model homogenous multiphase flow.

2.2.1.2.3. The Eulerian Model:

The Eulerian model is the most complex of the multiphase models. It solves a set of n momentum and continuity equations for each phase. Couplings are achieved through the pressure and inter phase exchange coefficients. The manner in which this coupling is handled depends upon the type of phases involved; granular (fluid-solid) flows are handled differently than non-granular (fluid-fluid) flows. For granular flows, the properties are obtained from application of kinetic theory. Momentum exchange between the phases is also dependent upon the type of mixture being modeled. Applications of the Eulerian Multiphase Model include bubble columns, risers, particle suspension, and fluidized beds.

2.2.2. Choosing a multiphase model

The first step in solving any multiphase problem is to determine which of the regimes best represent the flow. General guidelines provides some broad guidelines for determining the

appropriate models for each regime, and detailed guidelines provides details about how to determine the degree of interphase coupling for flows involving bubbles , droplets or particles , and the appropriate models for different amounts of coupling. In general, once that the flow regime is determined, the best representation for a multiphase system can be selected using appropriate model based on following guidelines. Additional details and guidelines for selecting the appropriate model for flows involving bubbles particles or droplets can be found.

- For bubble, droplet and particle-laden flows in which dispersed-phase volume fractions are less than or equal to 10% use the discrete phase model.
- For bubble, droplet and particle-laden flows in which the phases mix and / or dispersed phase volume fractions exceed 10% use either the mixture model.
- For slug flow, use the VOF model.
- For stratified / free-surface flows, use the VOF model.
- For pneumatic transport use the mixture model for homogenous flow or the Eulerian Model for granular flow.
- For fluidized bed, use the Eulerian Model for granular flow.
- For slurry flows and hydro transport, use Eulerian or Mixture model.
- For sedimentation, use Eulerian Model.

Depending on above guidelines following approach was chosen to carry out the simulation of fluidized bed.

CHAPTER 3

CFD SIMULATION OF GAS-LIQUID-SOLID FLUIDIZED BED

3.1. Computational flow model

In the present work, an Eulerian multi-fluid model is adopted where gas, liquid and solid phases are all treated as continua, inter- penetrating and interacting with each other everywhere in the computational domain. The pressure field is assumed to be shared by all the three phases, in proportion to their volume fraction. The motion of each phase is governed by respective mass and momentum conservation equations.

3.1.1. Equations

Continuity equation:

$$\frac{\partial}{\partial t}(\varepsilon_k \rho_k) + \nabla(\rho_k \varepsilon_k \vec{u}_k) = 0$$

Where ρ_k is the density and ε_k is the volume fraction of phase k=g, s, l and the volume fraction of the three phases satisfy the following condition:

$\varepsilon_g + \varepsilon_l + \varepsilon_s = 1$

Momentum equations:

For liquid phase:

$$\frac{\partial}{\partial t}(\rho_l \varepsilon_l \vec{u}_l) + \nabla(\rho_l \varepsilon_l \vec{u}_l \vec{u}_l)$$
$$= -\varepsilon_l \nabla P + \nabla(\varepsilon_l \mu_{\text{eff},l}(\nabla \vec{u}_l + (\nabla \vec{u}_l)^T)) + \rho_l \varepsilon_l g + M_{i,l}$$

For gas phase:

$$\frac{\partial}{\partial t}(\rho_g \varepsilon_g \vec{u}_g) + \nabla(\rho_g \varepsilon_g \vec{u}_g \vec{u}_g)$$
$$= -\varepsilon_g \nabla P + \nabla(\varepsilon_g \mu_{\text{eff},g}(\nabla \vec{u}_g + (\nabla \vec{u}_g)^T)) + \rho_g \varepsilon_g g - M_{i,g}$$

For solid phase:

$$\frac{\partial}{\partial t}(\rho_s \varepsilon_s \vec{u}_s) + \nabla(\rho_s \varepsilon_s \vec{u}_s \vec{u}_s)$$

where P is the pressure and μ_{eff} is the effective viscosity. The second term on the R.H.S of solid phase momentum equation is the term that accounts for additional solid pressure due to

solid collisions. The terms $M_{i,l}$, $M_{i,g}$, and $M_{i,s}$ of the above momentum equations represent the interphase force term for liquid, gas and solid phase, respectively.

3.1.2. Turbulence modelling:

Additional transport equations for the turbulent kinetic energy k and its dissipation rate ε were considered: the realizable k–ε model was chosen for modelling the turbulence. It joins the properties of the standard k–ε model, such as robustness and reasonable accuracy for a wide range of industrial applications, with recently developed model improvements that provide better performance in the presence of jets and mixing layers. The upgrading concerns the formulation of the turbulent viscosity and the transport equation for ε (Shih et al., 1995).

k–ε models assume a high Reynolds number and fully turbulent flow regime so auxiliary methods are required to model the transition from the thin viscous sub-layer flow region along a wall to the fully turbulent, free stream flow region. The choice of the ‘‘standard walls function’’ approach determines that the viscosity affecting the near-wall region is not resolved. Instead, analytical expressions are used to bridge the wall boundary and the fully turbulent flow field: the expression implemented in FLUENT is the logarithmic law of the wall for velocity; corresponding relations are available for temperature and wall heat flux. Wall functions avoid the turbulence model adaptation to the presence of the wall, saving computational resources.

3.2. Problem description:

The problem consists of a three phase fluidized bed in which air and liquid (water) enters at the bottom of the domain. The bed consists of solid material (Glass beads) of uniform diameter which forms a desired height in the bed.

Table.2.Properties of air, water and glass beads used in experiment

Phases	Density	Viscosity
Air	1.225 Kg/m^3	$1.789*10^{-05}$ kg/m-s
Water	998.2 Kg/m^3	0.001003 kg/m-s
Glass beads	2470 kg/m^3	Same as water

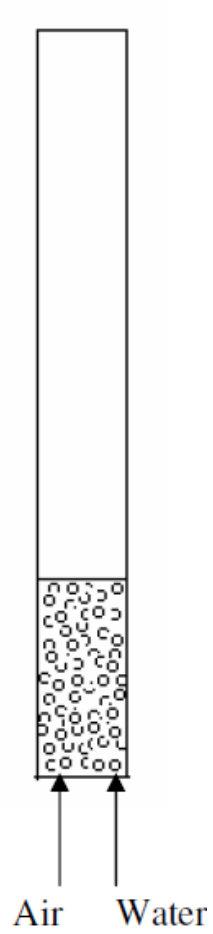

Fig.5. Experimental setup of fluidized bed column used (Static bed heights=17.1cm, 21.3cm)

3.3. Simulation:

3.3.1. Geometry and Mesh

GAMBIT 2.2.30 was used for making 2D rectangular geometry with width of 0.1m and height 1.88m. Coarse mesh size of 0.01m was taken in order to have 1880 cells (3958 faces) for the whole geometry. Similarly a mesh size of 0.005 cm was also used in order to have better accuracy. But using fine mesh results in 7520 cells (15436 faces), which requires smaller time steps, more number of iterations per time step and 4 times more calculation per iteration for the solution to converge. Also because results obtained in case of coarse grid were in good accordance with experimental outputs, coarse grid was preferred over finer grid for simulation. Figure # shows two types of meshing.

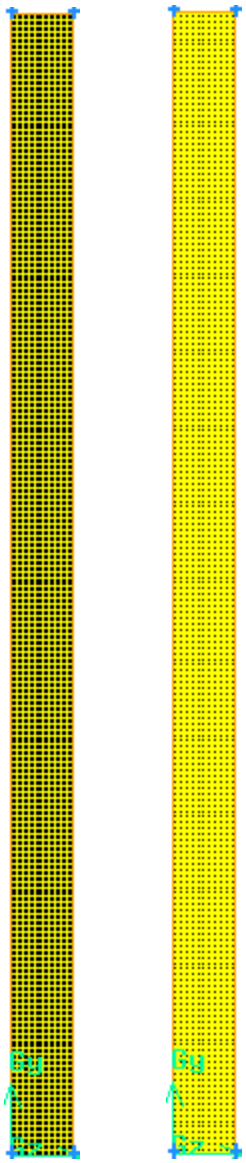

Fig.6. Coarse mesh (left) and fine mesh (right) created in GAMBIT

3.3.2. Selection of models for simulation:

FLUENT 6.2.16 was used for simulation. 2D segregated 1st order implicit unsteady solver is used.(The segregated solver must be used for multiphase calculations). Standard k-ε dispersed eulerian multiphase model with standard wall functions were used.

The model constants are tabulated as:

Table.3. Model constants used for simulation

Cmu	0.09
C1-Epsilon	1.44
C2-Epsilon	1.92
C3-Epsilon	1.3
TKE Prandtl Number	1
TDR Prandtl Number	1.3
Dispersion Prandtl Number	0.75

Water is taken as continuous phase while glass and air as dispersed phase. Inter-phase interactions formulations used were

- Liquid – Air: schiller-naumann
- Solid-Liquid: Gidaspow
- Solid-Air:Gidaspow

Air velocities ranging from 0.0125m/s to 0.1m/s with increment of 0.0125 and water velocities from 0 to 0.17m/s with inlet air volume fractions obtained as fraction of air entering in a mixture of gas and liquid were the parameters used for boundary conditions.

Pressure outlet boundary conditions :

Mixture Gauge Pressure- 0 pascal.

Solid and liquid Boundary Conditions.

Backflow Total Temperature- 293.

Backflow Granular Temperature -0.0001.

Backflow Volume Fraction- 0.

Specified shear was set as X=0 and Y=0 for gas and solid whereas no slip condition for water was used.

3.3.3. Solution:

Under relaxation factor for pressure, momentum and volume fraction were taken as 0.3, 0.2, and 0.5 respectively. The discretization scheme for momentum, volume fraction, turbulence kinetic energy and turbulence dissipation rate were all first order upwind. Pressure-velocity coupling scheme was Phase Coupled SIMPLE. The solution was initialized from all zones. For patching a solid volume fraction calculated from experimental settings i.e. the volume fraction of solid in the part of the column up to which the glass beads were fed was used. Iterations were carried out for time step size of 0.01-0.001 depending on ease of convergence and time required to get the result for fluidization.

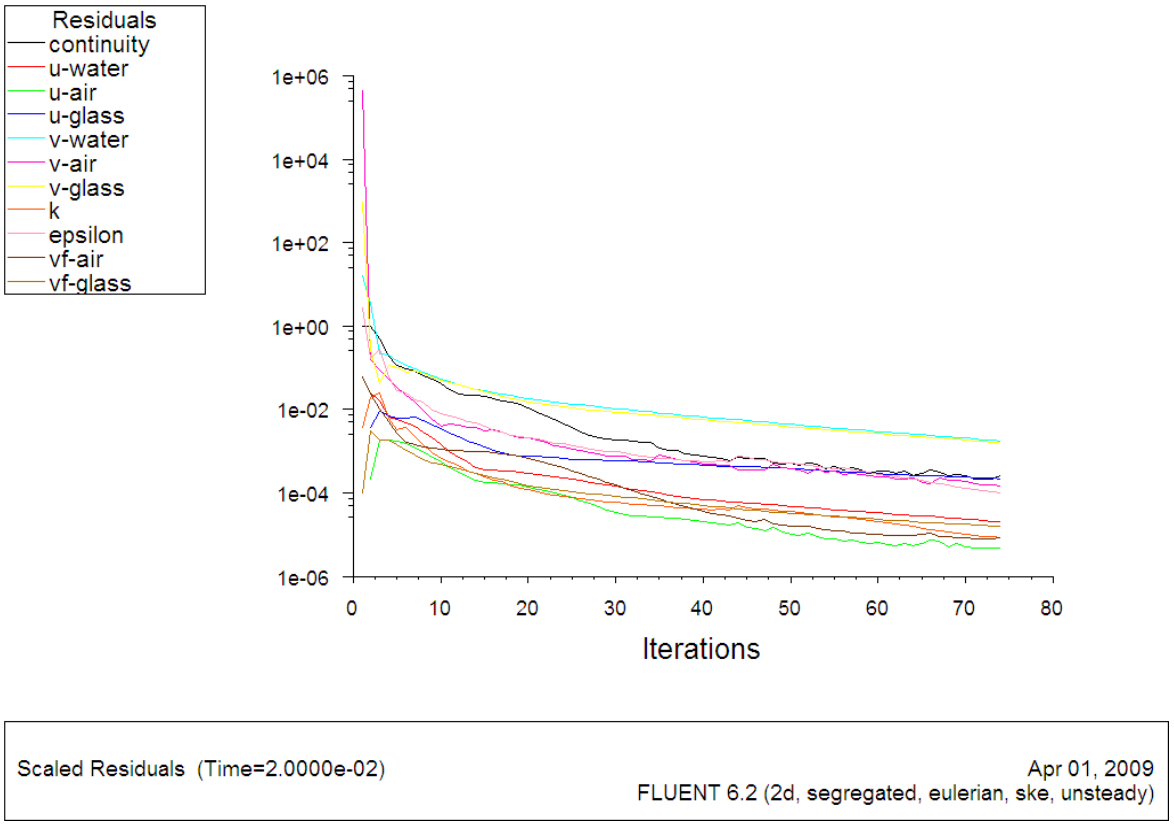

Fig.7. Plot of residuals for k-epsilon solver method as the iterations proceeds.

Convergence and accuracy is important during solution. This can be seen by the residual plots in fig.7.. A convergence criterion of 10^{-3} is taken here. If not then we have to change the solution parameters and sometimes solution method also. Currently, K-epsilon method is used for the hydrodynamic study of the fluidized bed.

CHAPTER 4

RESULTS AND DISCUSSION

A gas-liquid-solid fluidized bed of diameter 0.1m and height 1.88m has been simulated using commercial CFD software package FLUENT 6.2.16. The simulation has been done for static bed heights of 17.1cm and 21.3cm with glass beads of diameter 2.18mm. The inlet superficial velocity of air ranges from 0.0125m/s to 0.1m/s while that of water ranges from 0.0m/s to 0.14 m/s. The results obtained have been presented graphically in this section.

While simulating the fluidized bed the profile of bed changes with time. But after some time no significant change in the profile is observed. This indicates that the fluidized bed has come to a quasi steady state. Contours of volume fraction of bed with respect to time of fluidization are shown in fig.8. Simulation should be carried out till there no significant change in the profile of bed; like that between 20 and 30 seconds.

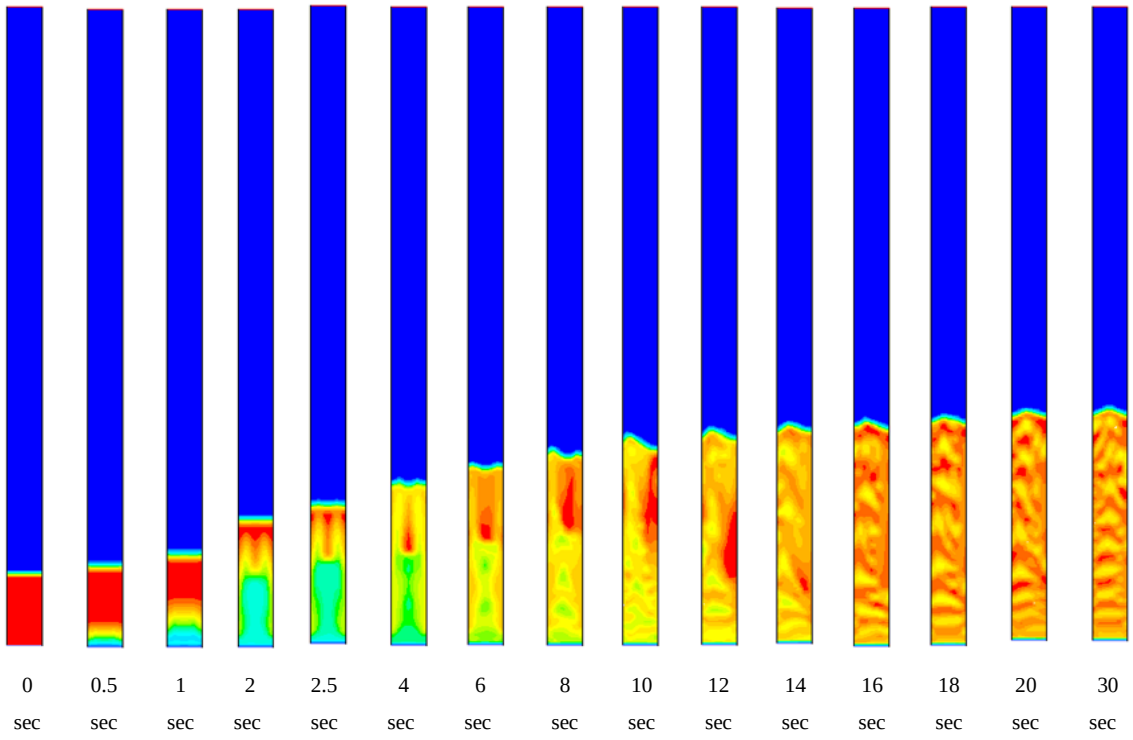

Fig.8. Contours of volume fraction of glass beads at water velocity of 0.12m/s and air velocity of 0.0125m/s with respect of time for initial bed height 21.3cm.

4.1. Phase Dynamics

Solid, liquid and gas phase dynamics has been represented in the form of contours, vectors and XY plots. Figure 9 shows the contours of volume fractions of solid, liquid and gas in the column obtained at water velocity of 0.12m/s and air velocity of 0.0125m/s for static bed height 21.3cm and glass beads of diameter 2.18mm after the quasi steady state is achieved. The color scale given to the left of each contours gives the value of volume fraction corresponding to the color. The contours for glass beads illustrates that bed is in fluidized condition. The contours for water illustrates that volume fraction of water (liquid holdup) is less in fluidized part of the column compared to remaining part. The contour for air illustrates that gas holdup is significantly more in fluidized part of the bed compared to remaining part.

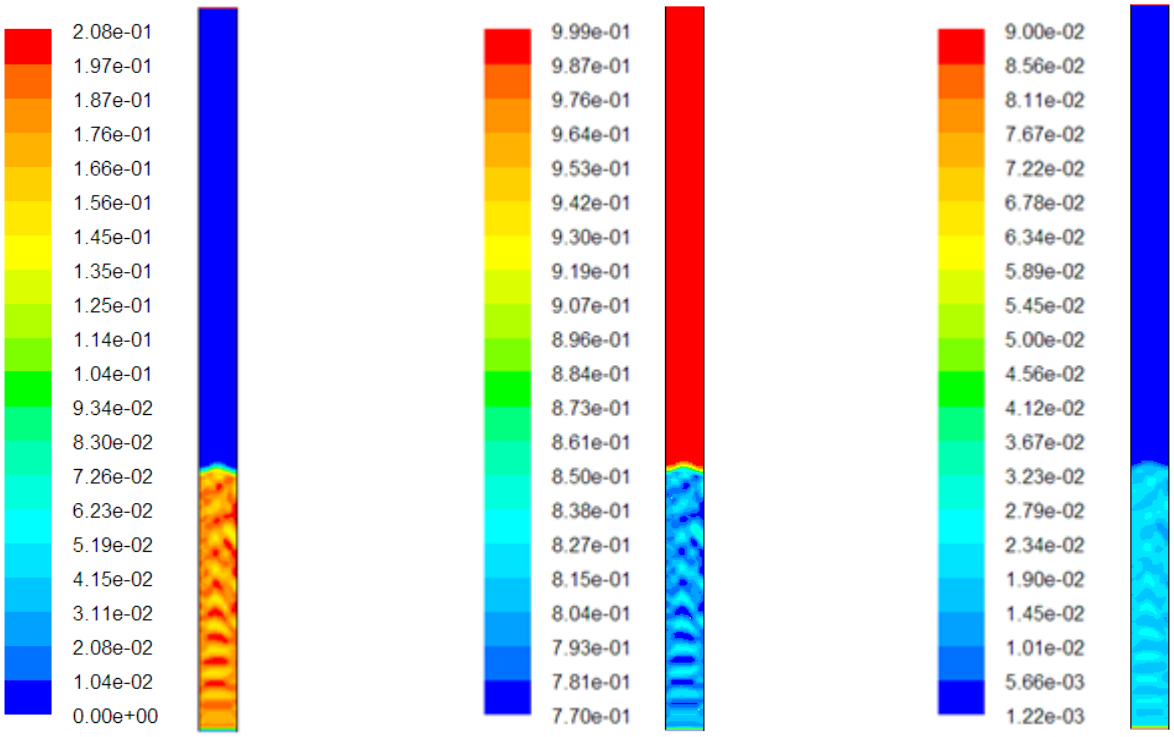

Fig.9. Contours of volume fractions of solid, liquid and gas at water velocity of 0.12m/s and air velocity of 0.0125m/s for initial bed height 21.3cm

Vectors of velocity magnitude of glass beads, water and air in the column obtained at inlet water velocity of 0.12m/s and inlet air velocity of 0.0125m/s for static bed height 21.3cm and glass beads of diameter 2.18mm after the quasi steady state is achieved are shown in figures 10-12. These vectors show velocity magnitude with direction and thus helpful in determining flow patterns in fluidized bed.

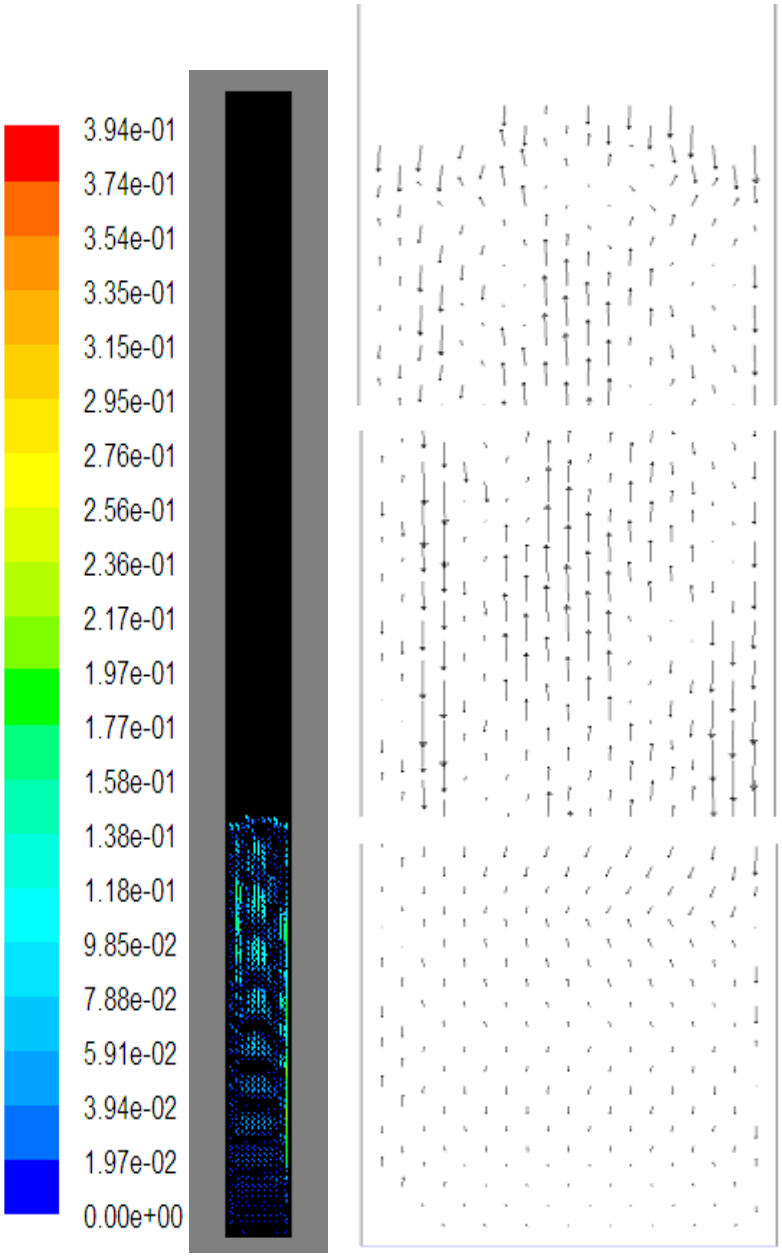

From figure 10 it can be clearly observed that the velocity at the bottom is small. In the middle expanded section of the bed we can see that near the wall direction of velocity is downwards while that in the zone away from wall the direction of velocity is upwards. Also at the top of the expanded part of the bed, all the velocity vectors are showing downward trend. Because no glass beds are present in the upper section, no velocity vectors can be seen.

Fig.10. Velocity vector of glass beads in the column (actual and magnified)

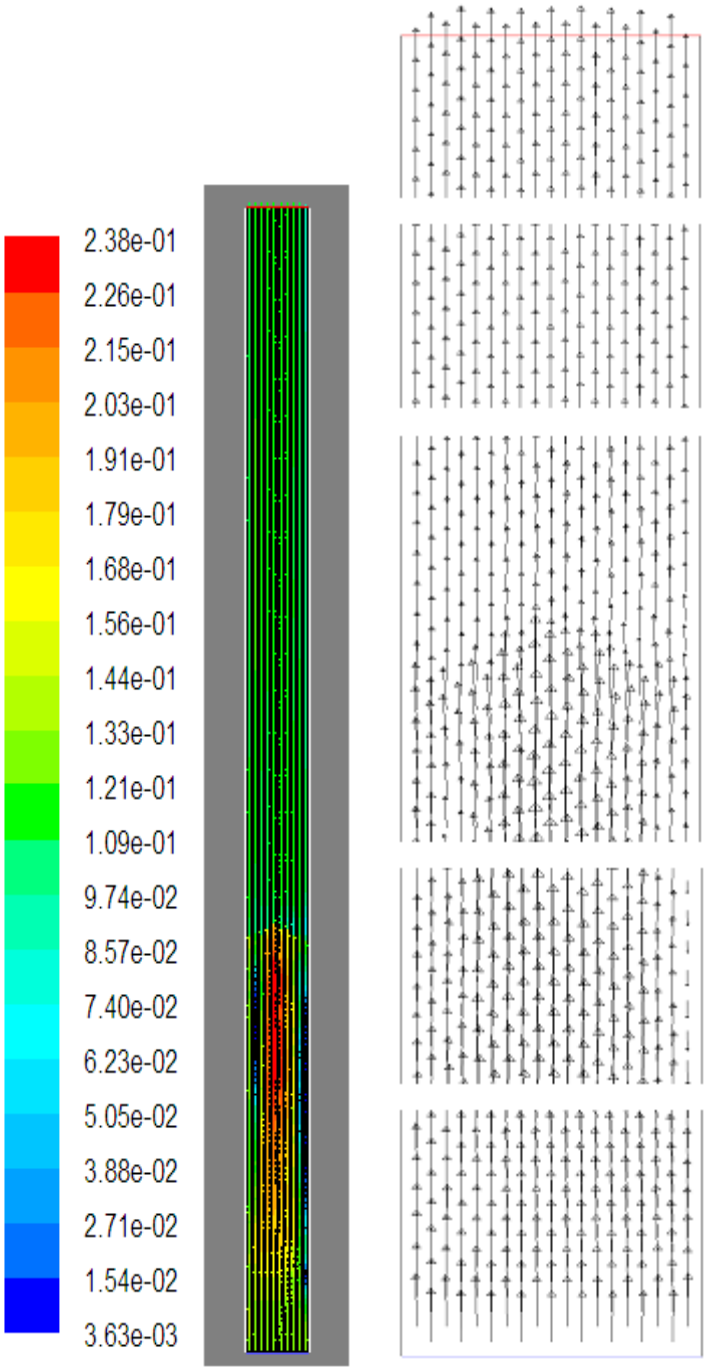

The velocity vector of water in the column as can be seen in figure 11 shows always an upward trend. However the velocity is more in fluidized section of the bed compared to the part of the column which contains no glass beads. This is because less space is available for water to flow. The transition from high to low velocity can be clearly seen when water leaves fluidized part of the bed.

Fig.11. Velocity vector of water in the column (actual and magnified**)**

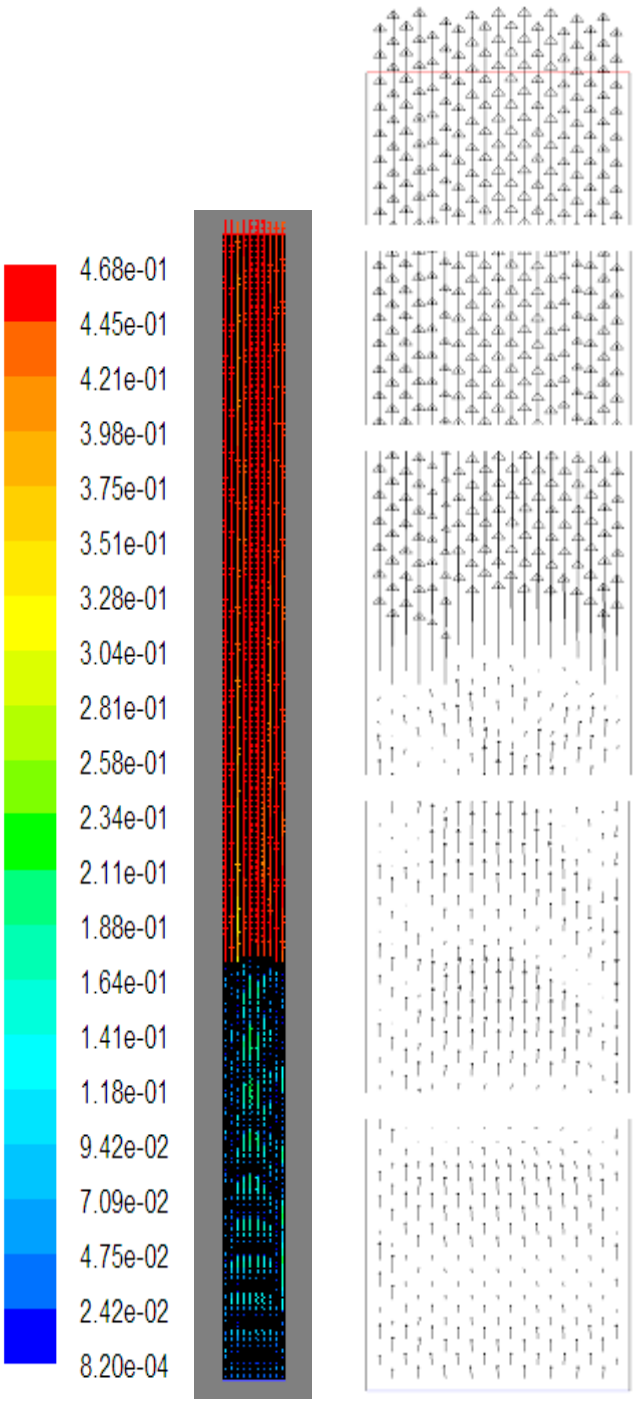

Here as it can be seen in figure 12 the velocity vectors show that velocity of air is very small in fluidized portion of the column compared to that in remaining part of the column. This is because of very small volume fraction of air compared to glass beads and water. This may also happen that glass beads obstruct the air bubbles thereby lowering its velocity. In the upper section of the column; water, whose velocity is high carries air bubbles, so velocity of air bubbles reduces.

Fig.12. Velocity vector of air in the column (actual and magnified)

Following are the XY plots of velocity magnitudes obtained at inlet water velocity of 0.12m/s and inlet air velocity of 0.0125m/s. For a fully developed flow this kind of parabolic pattern is must. Besides, following figures also gives maximum outlet velocity of water about 0.14m/s and that of air about 0.48m/s. Also velocities at wall are zero.

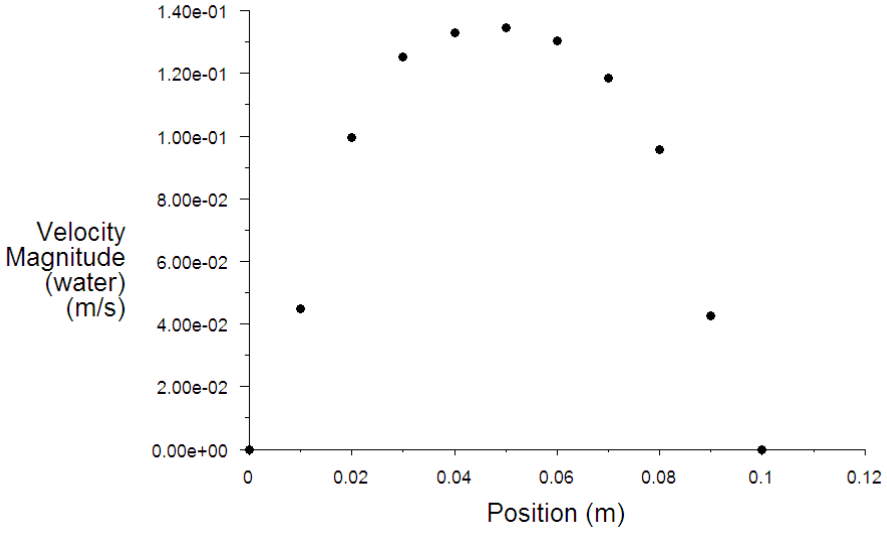

Fig.13. XY plot of velocity magnitude of water

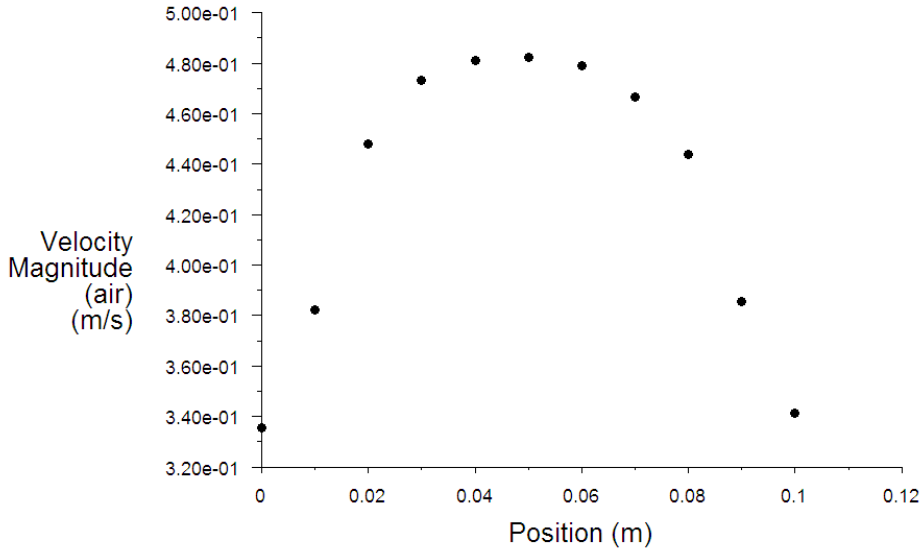

Fig.14. XY plot of velocity magnitude of air

4.2. Bed Expansion

Figure 15 shows a set of contours of solid volume fraction at inlet air velocity 0.05m/s and different inlet water velocities for initial bed height 17.1 cm and glass beads of size 2.18mm. These contours show that bed expands as liquid velocity increases at constant gas velocity.

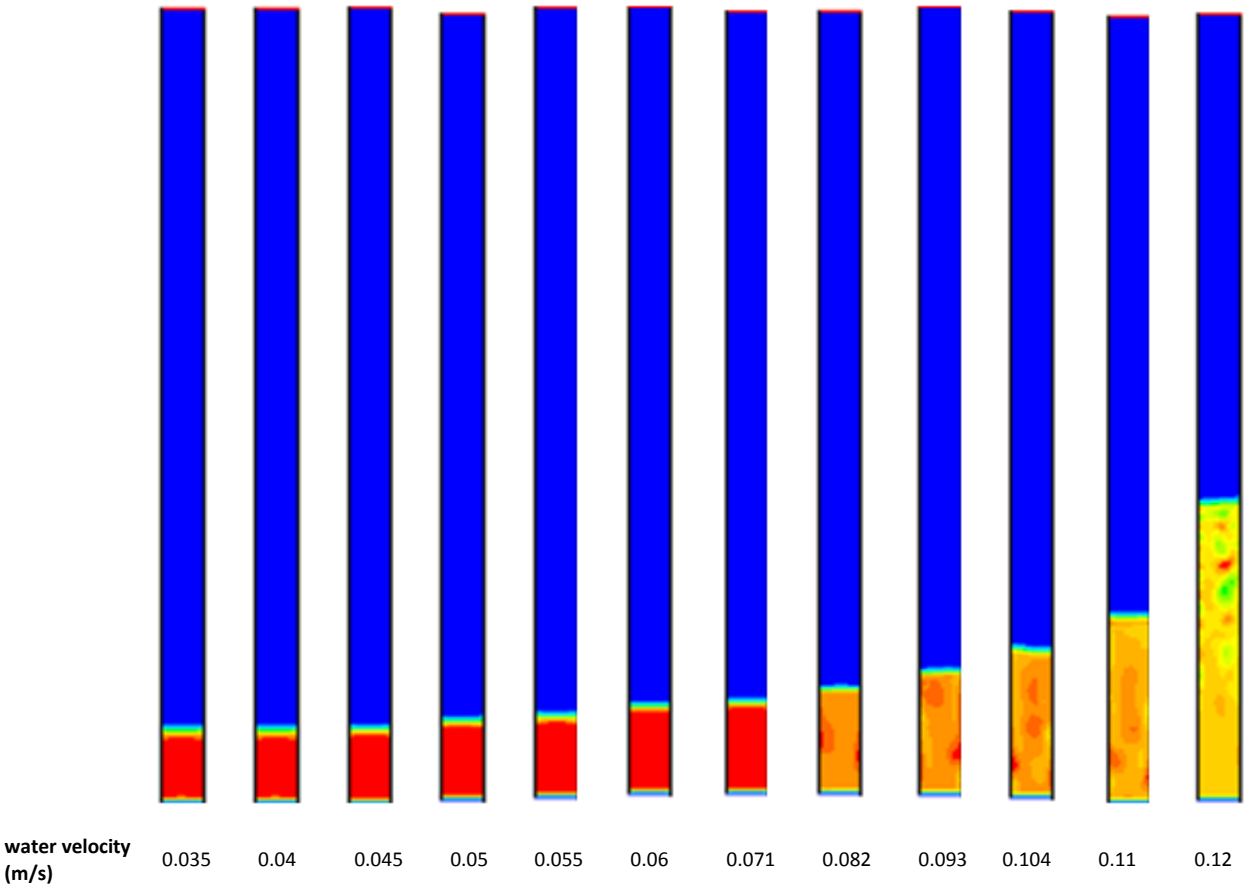

Fig.15. Contours of volume fraction of glass beads with increasing water velocity at inlet air velocity 0.05m/s for initial bed height 17.1cm and glass beads of size 2.18mm

Bed height is determined by taking an X-Y plot of volume fraction of glass beads on Y-axis while height of the column at X-axis. Example:

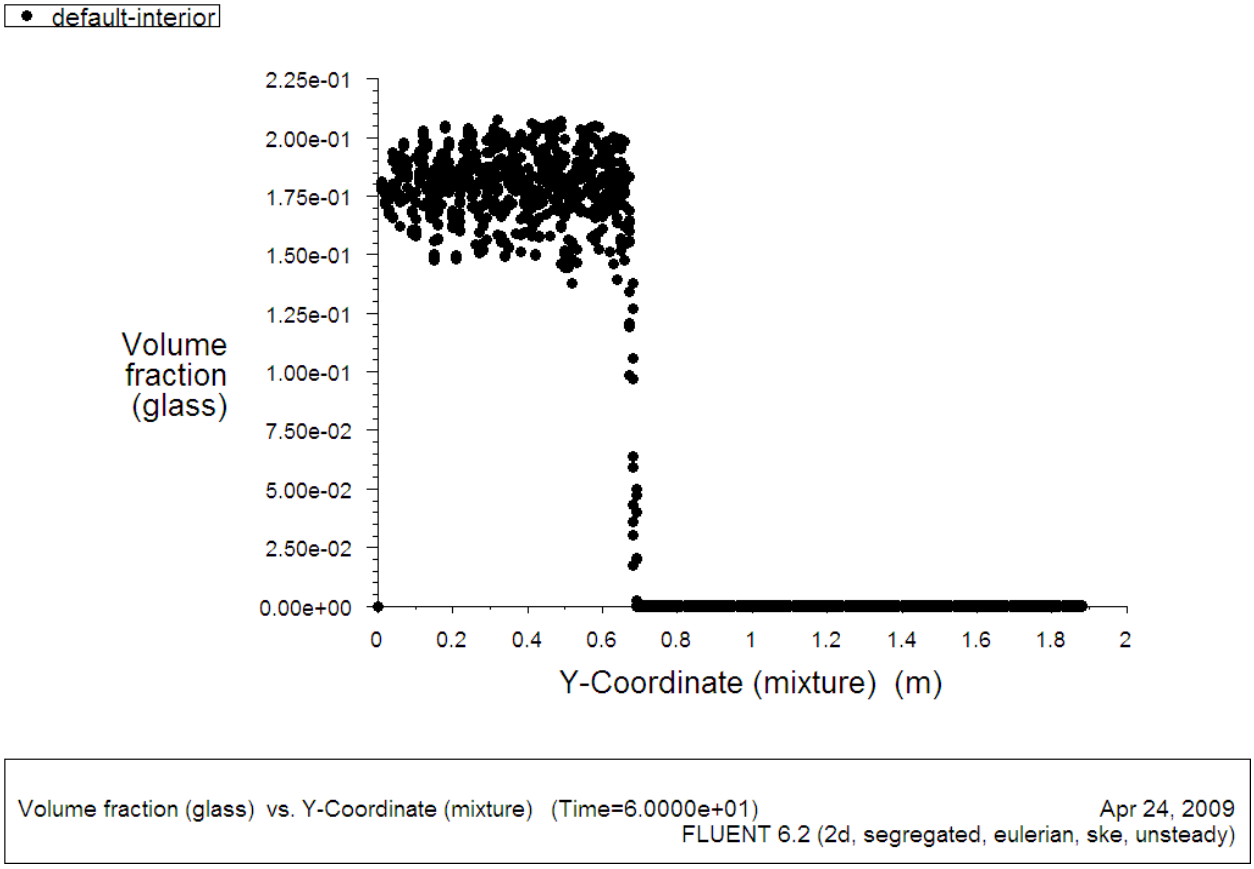

Fig.16. X-Y plot of volume fraction of glass beads

Following are the trends of bed expansion vs. inlet water velocity obtained at different inlet air velocities, which show that bed expands when water velocity increases.

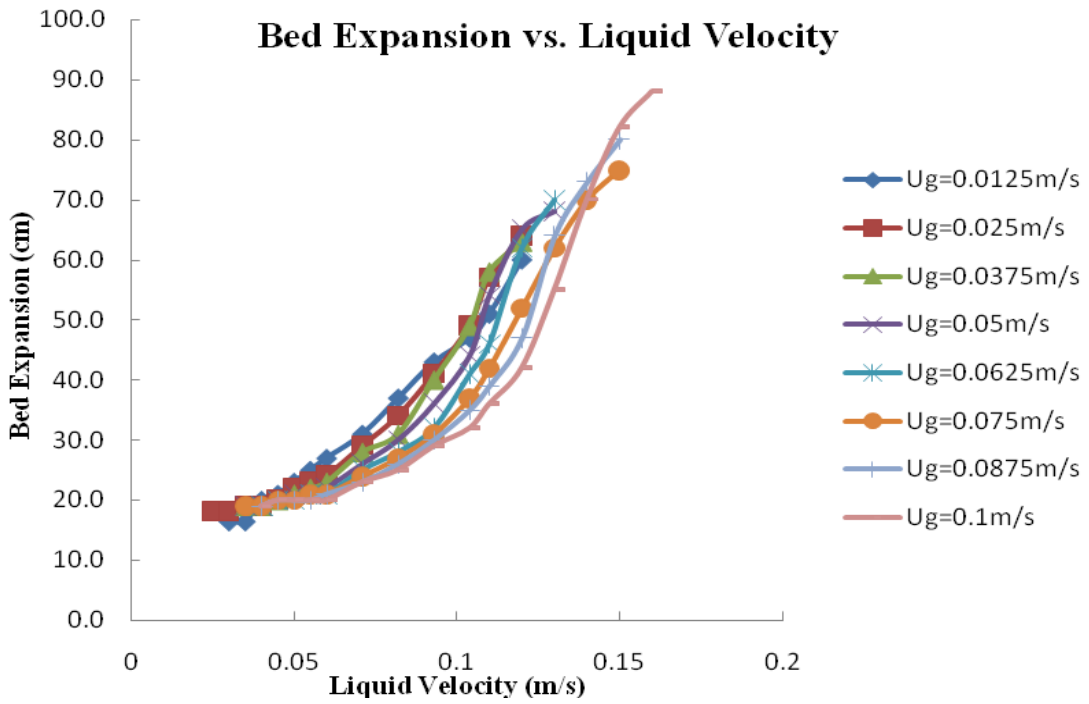

Fig.17. Bed expansion vs. water velocity for initial bed height 17.1cm and particle size 2.18mm

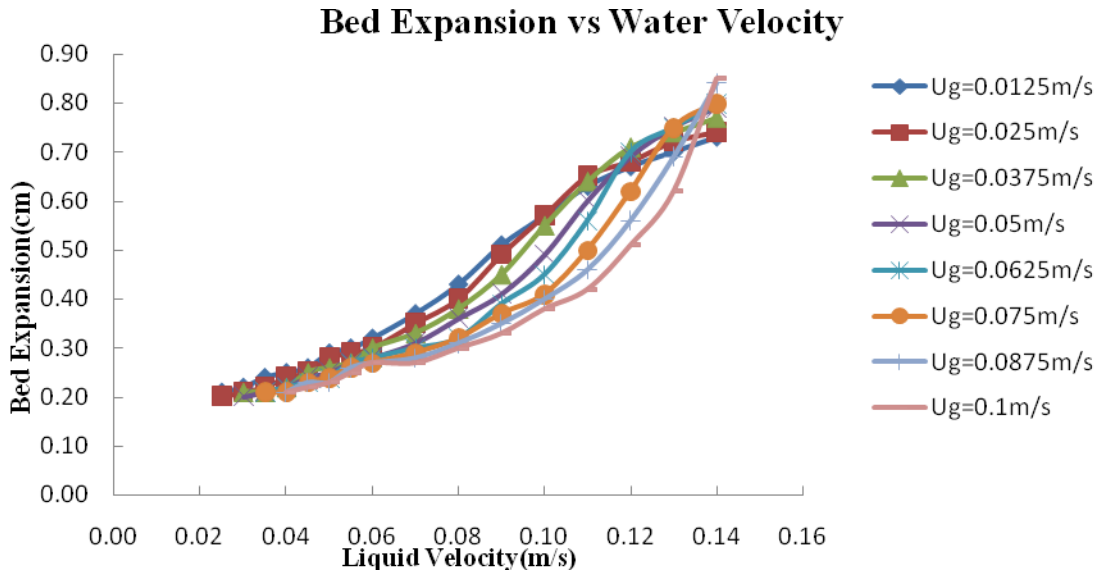

Fig.18. Bed expansion vs. water velocity for initial bed height 21.3cm and particle size 2.18mm

Next is shown a comparison of experimental results and simulated results obtained at air velocity 0.05m/s and initial bed height 17.1 cm. It is clear that simulated results are in excellent agreement with experimental results and there is hardly a difference of 1% or so.

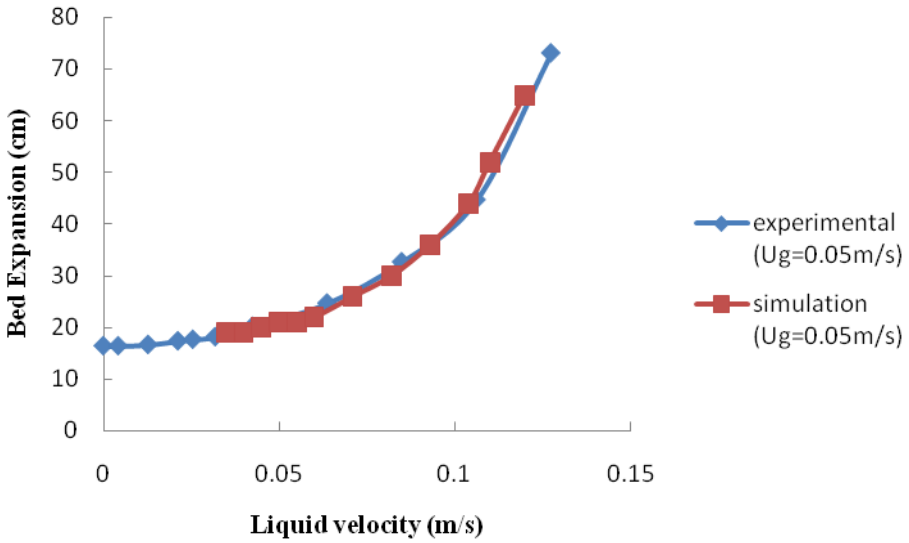

Fig.19. Comparison of experimental results and simulated results obtained at air velocity 0.05m/s and initial bed height 17.1 cm

4.3. Gas Holdup

Gas holdup is obtained as mean area-weighted average of volume fraction of air at sufficient number of points in fluidized part of the bed. As shown in the adjoining figure 20 volume fraction of air phase is not the same at all points in fluidized part of the column. Hence area weighted average of volume fraction of air is determined at heights 10cm, 20 cm 30 cm etc till fluidized part is over. When these values are averaged gives the required gas holdup.

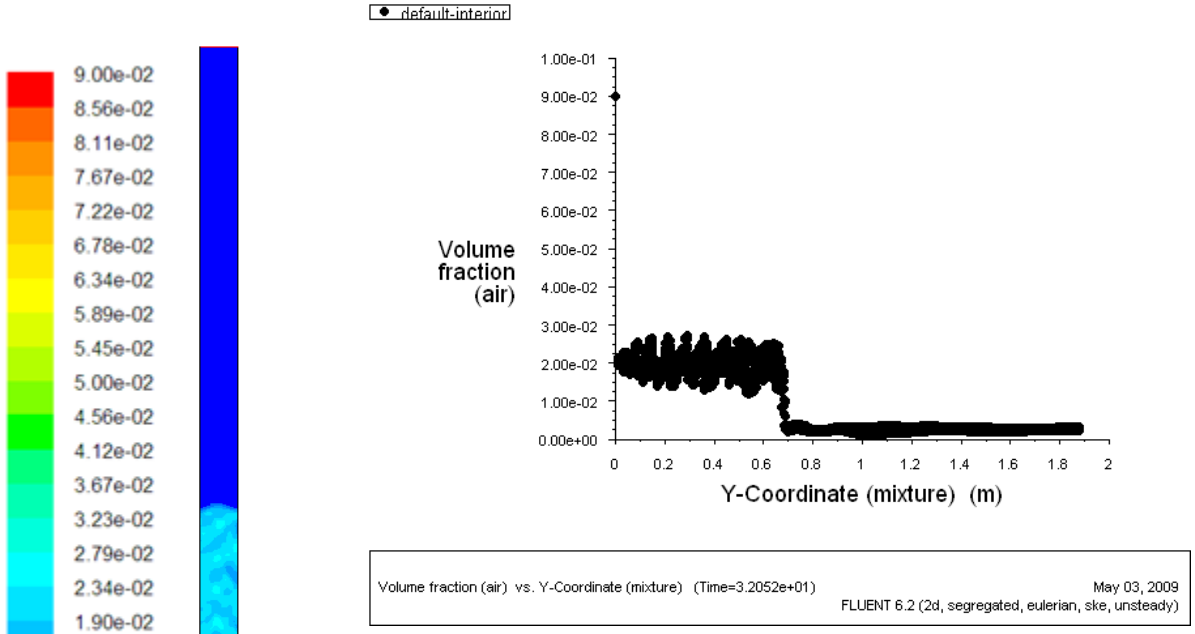

Fig.20. Contour (left) and XY plot (right) of air volume fraction at water velocity of 0.12m/s and air velocity of 0.0125m/s for initial bed height 21.3cm

Following are the trends of gas holdup vs. inlet water velocity obtained at different inlet air velocities, which show that gas holdup decreases when water velocity is increased.

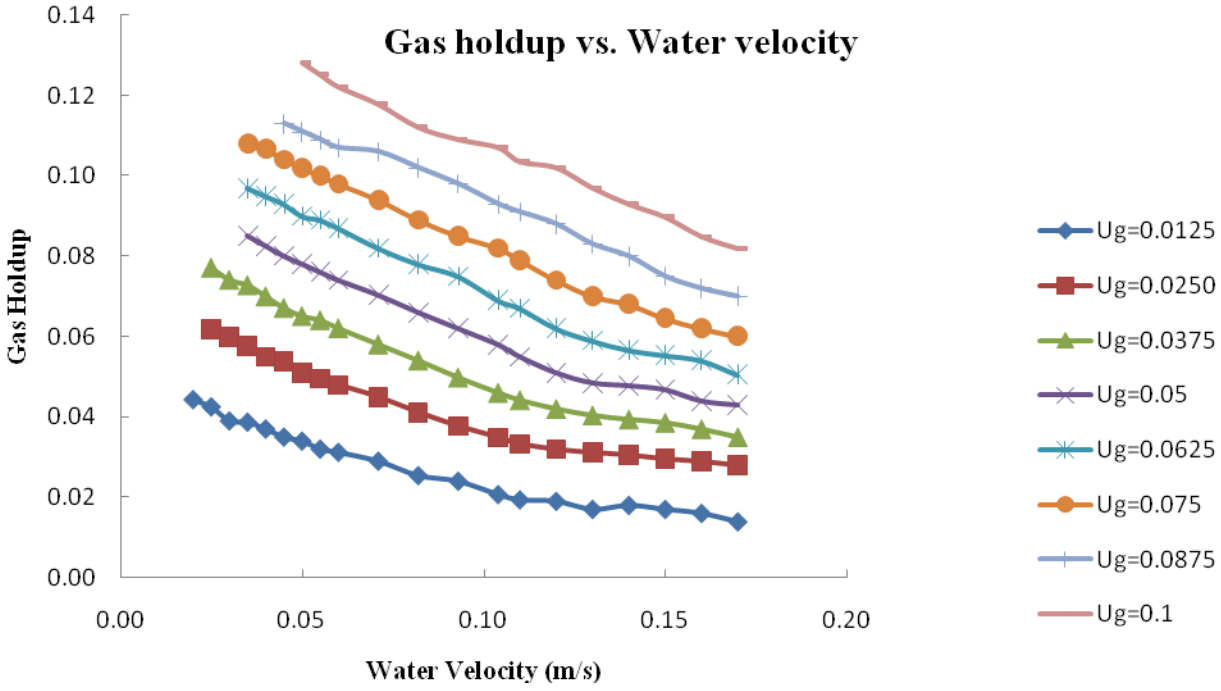

Fig.21. Gas holdup vs. water velocity for initial bed height 17.1 cm and particle size 2.18mm

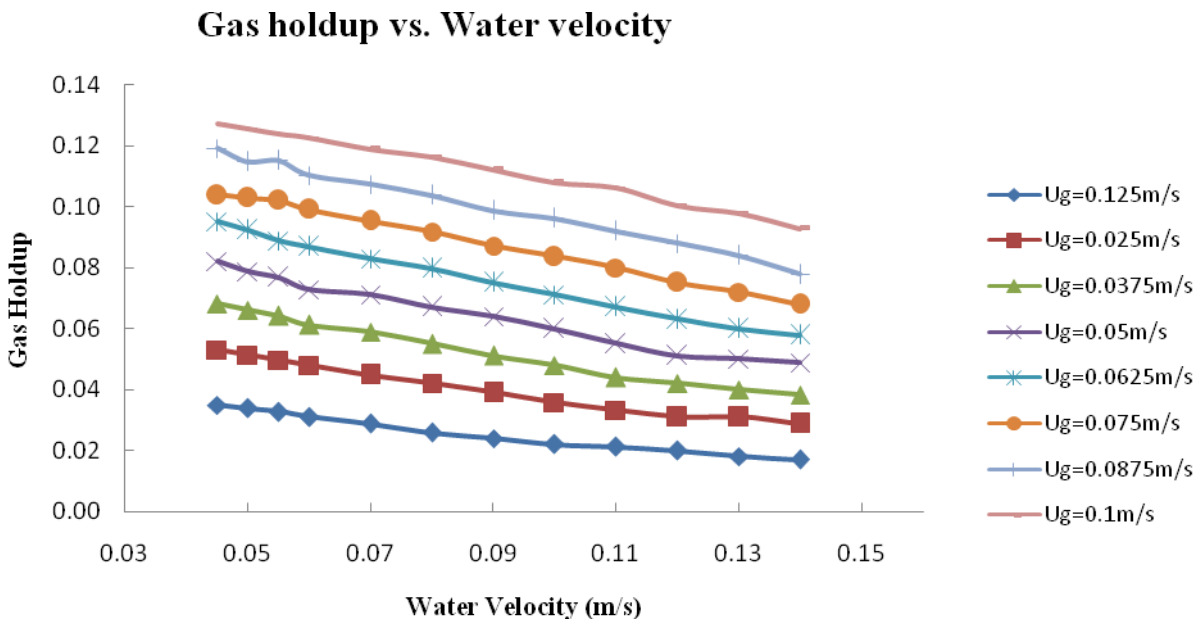

Fig.22. Gas holdup vs. water velocity for initial bed height 21.3 cm and particle size 2.18mm

Following are the trends of gas holdup vs. inlet air velocity obtained at different inlet water velocities, which show that gas holdup increases when air velocity is increased.

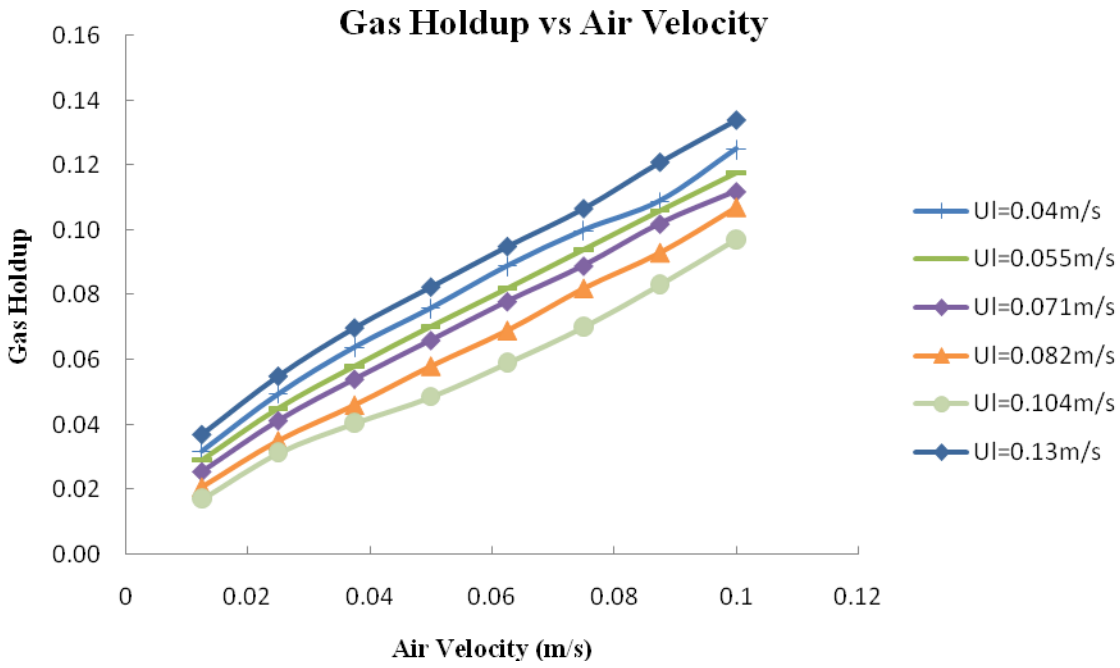

Fig.23. Gas holdup vs. water velocity for initial bed height 17.1 cm and particle size 2.18mm

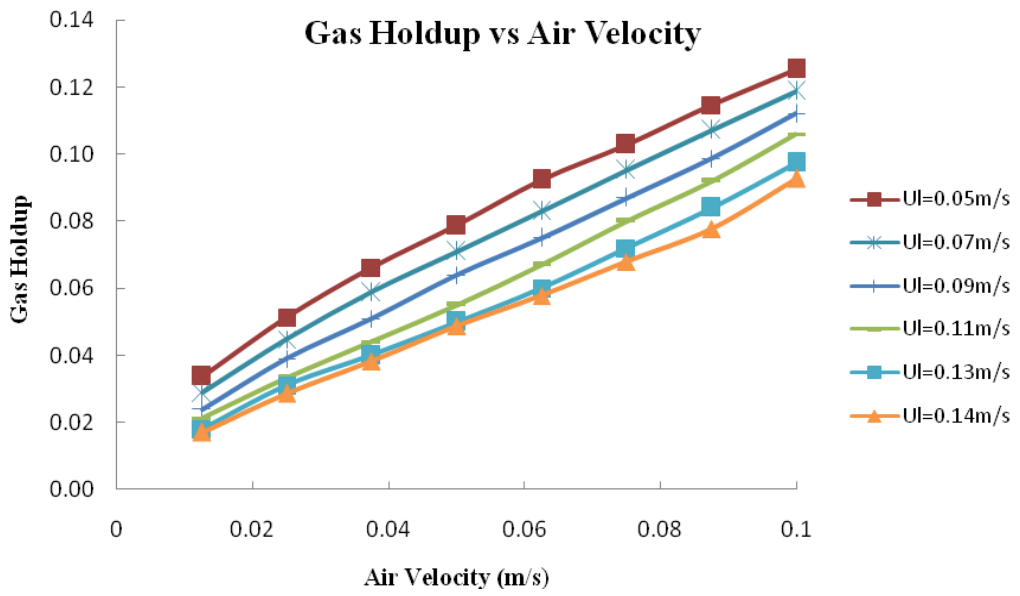

Fig.24. Gas holdup vs. air velocity for initial bed height 21.3 cm and particle size 2.18mm

Following is the plot showing comparison of experimental result of gas holdup with that of simulated result obtained at air inlet velocities 0.025 m/s and 0.05m/s for initial bed height 21.3 cm. It shows that in both the conditions simulated results are in excellent agreement with experimental results with deviation of less than 5%. The reason for small deviation may be that the glass beads used in experiment have a range of diameters while in the simulation all glass beads are taken to be of the same diameter.

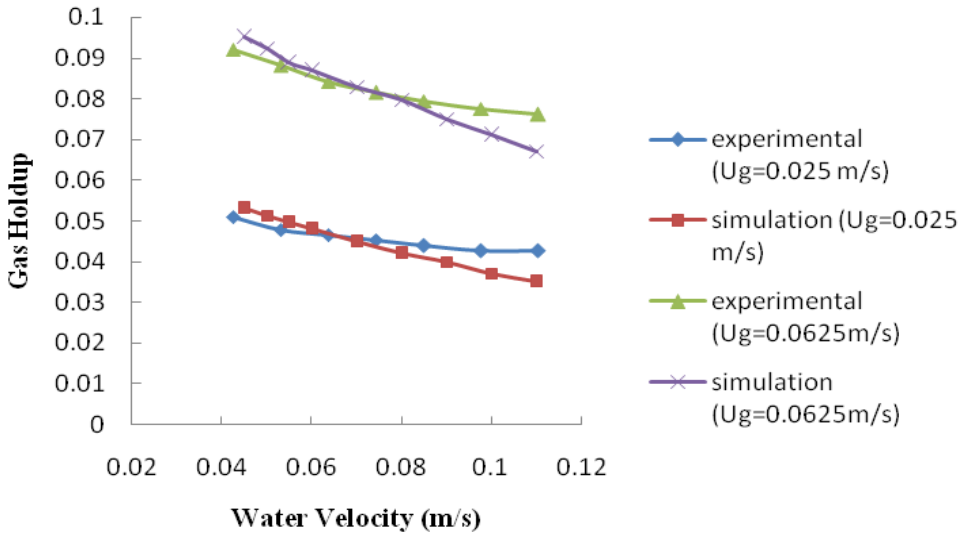

Fig.25. Comparison of experimental result of gas holdup with that of simulated result obtained at air inlet velocities 0.025 m/s and 0.05m/s for initial bed height 21.3 cm

4.4. Pressure Drop

Following are the contours of static gauge pressure (mixture phase) in the column obtained at water velocity of 0.12m/s and air velocity of 0.0125m/s. This contour illustrates that pressure increases as we move from top to bottom. Also pressure at inlet and outlet can be determined which is helpful in finding the pressure drop across the column.

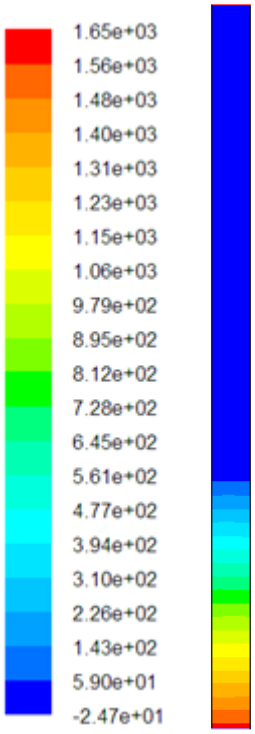

Fig.26. Contours of static gauge pressure (mixture phase) in the column obtained at water velocity of 0.12m/s and air velocity of 0.0125m/s.

Following are the trends of pressure drop vs. water velocity obtained at different inlet air velocities, which show that pressure drop increases when water velocity is increased. Also when the air velocity is small (U_g=0.0125 m/s) there is no substantial increase in pressure drop. This can be attributed to the fact that at small air velocity, the operation becomes almost solid-liquid

fluidization because of small inlet volume fraction of the air compared to that of water.

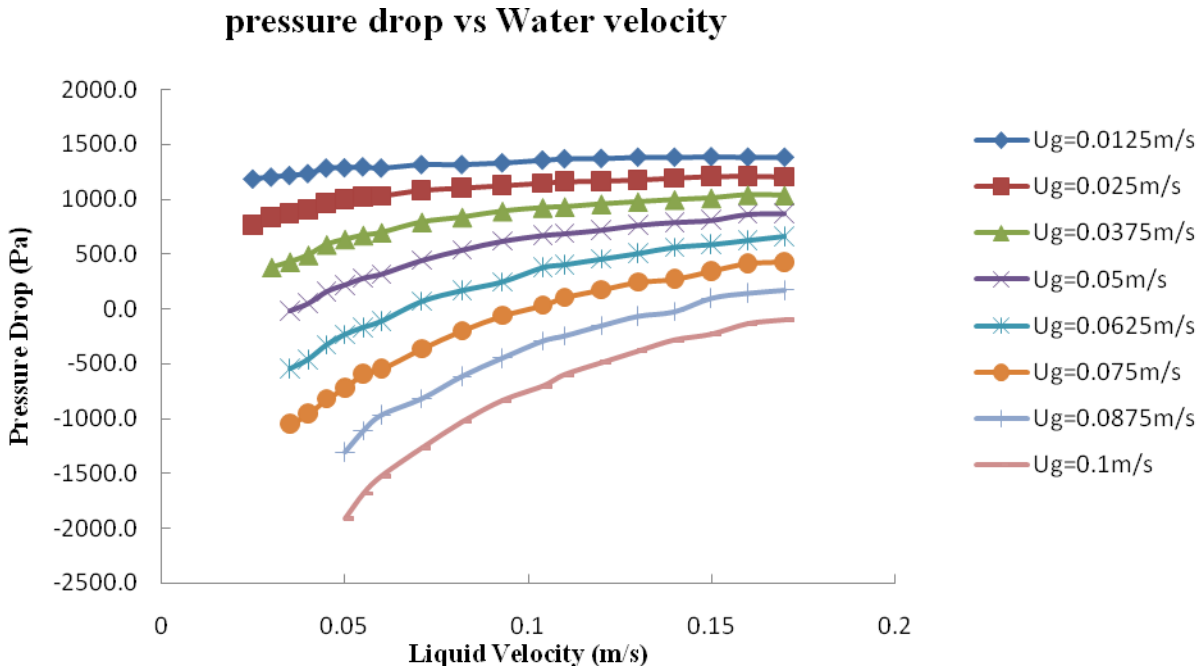

Fig.27. Pressure Drop vs. water velocity for initial bed height 17.1 cm and particle size 2.18mm

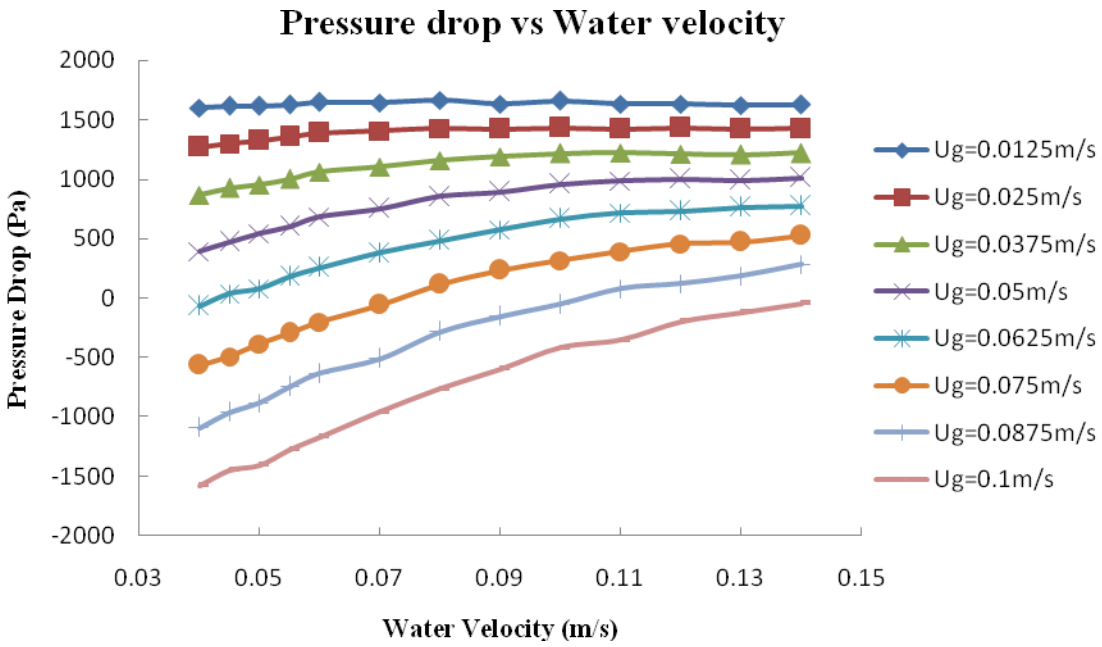

Fig.28. Pressure Drop vs. water velocity for initial bed height 21.3 cm and particle size 2.18 mm

Following plots of pressure drop vs. inlet air velocity obtained at different inlet water velocity show that pressure drop decreases as air velocity is increased. This is because with increase in air velocity the hold up of water in the column decreases (whose density is much larger compared to that of air) thereby decreasing the pressure drop across the column.

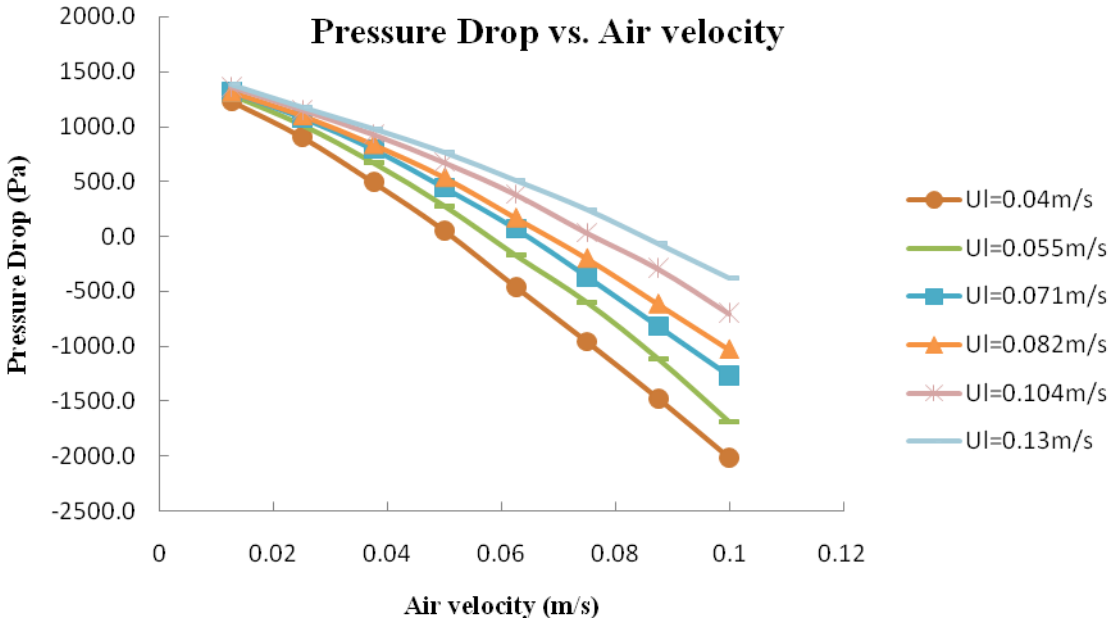

Fig.29. Pressure Drop vs. Air velocity for initial bed height 17.1 cm and particle size 2.18mm

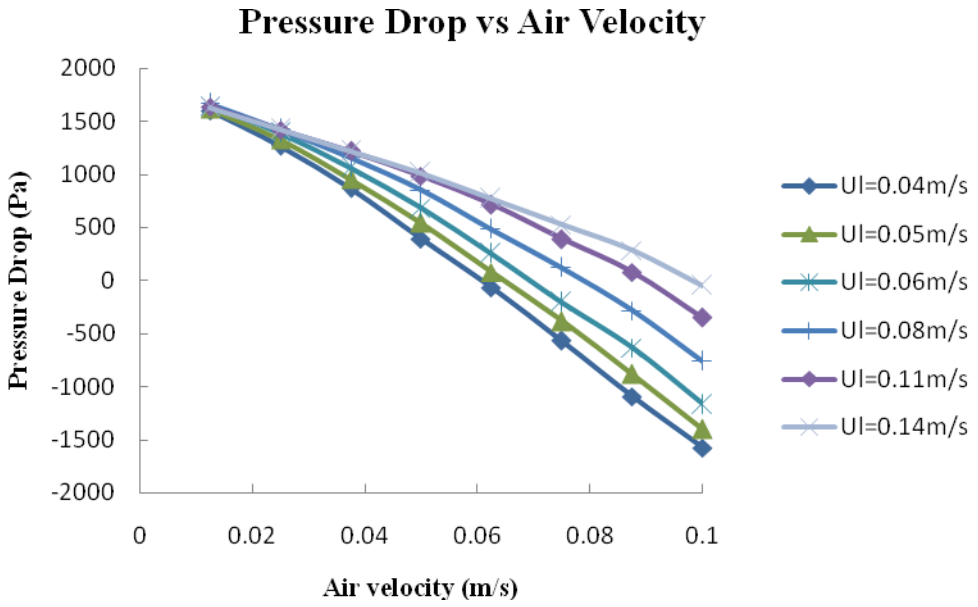

Fig.30. Pressure Drop vs. Air velocity for initial bed height 21.3 cm and particle size 2.18mm

Following is shown a comparison between pressure drop from experiment and that from simulation at air inlet velocity 0.025 m/s and 0.025 m/s for initial bed height 21.3 cm. The results obtained from simulation differ from experiment only by 10% or less. The reason for this small deviation may be that the glass beads used in experiment have a range of diameters while in the simulation all glass beads are taken to be of the same diameter.

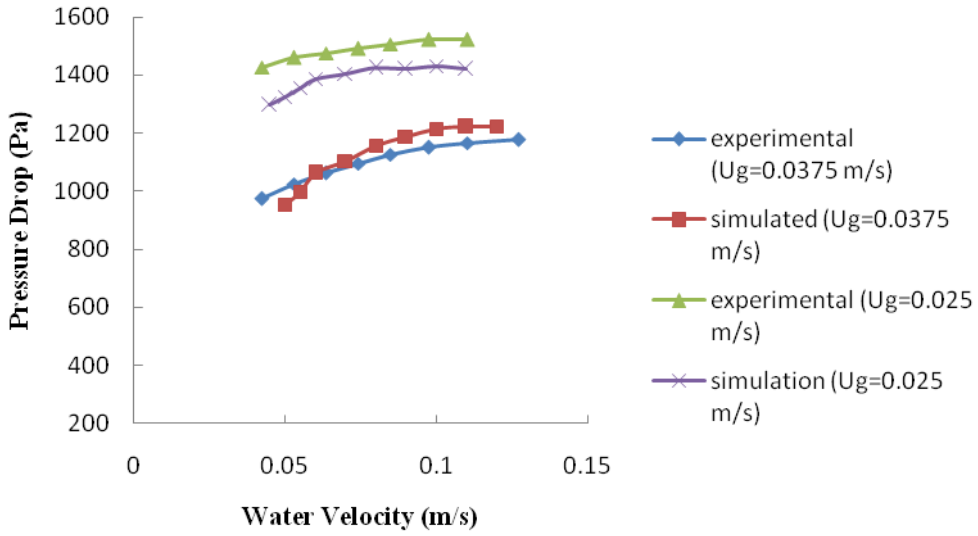

Fig.31. Comparison between pressure drop from experiment and that from simulation at air inlet velocity 0.025 m/s and 0.025 m/s for initial bed height 21.3 cm

CHAPTER 5

CONCLUSION

1. Trends of bed expansion vs. inlet water velocity obtained at different inlet air velocities show that bed expands when water velocity increases.

2. Trends of gas holdup vs. inlet water velocity obtained at different inlet air velocities show that gas holdup decreases when water velocity is increased.

3. Trends of gas holdup vs. inlet air velocity obtained at different inlet water velocities show that gas holdup increases when air velocity is increased.

4. Trends of pressure drop vs. water velocity obtained at different inlet air velocities show that pressure drop increases when water velocity is increased. Also when the air velocity is small (U_g=0.0125 m/s) there is no substantial increase in pressure drop. This can be attributed to the fact that at small air velocity, the operation becomes almost solid-liquid fluidization because of small inlet volume fraction of the air compared to that of water.

5. Plots of pressure drop vs. inlet air velocity obtained at different inlet water velocity show that pressure drop decreases as air velocity is increased. This is because with increase in air velocity the hold up of water in the column decreases (whose density is much larger compared to that of air) thereby decreasing the pressure drop across the column.

6. The pressure drop is influenced by the initial static bed height. This is low for small initial bed height compared to higher initial bed height.

7. Since the bed expansion, gas holdup and pressure drop data obtained from simulation are showing very small deviation from experimental results, therefore CFD model developed in this work can be taken as very good approximation of gas-liquid-solid fluidized bed.

References:

1. L. S. Fan, Gas–Liquid–Solid Fluidization Engineering, Butterworth-Heinemann, Boston, 1989

2. Bigot, V., Guyot I. Bataille D., Roustan M., "Possibilities of use of two sensors depression metrological techniques and fiber optics, to characterize the hydrodynamics of a fluidised bed triphasic", In: Stork, A., Wild, G. (Eds.), Recent Advances in Process Engineering, vol. 4 (1990). pp. 143-1

3. Merchant F.J.A., Margaritis A., Wallace J.B., "A novel technique for measuring solute diffusivities in entrapment matrices used in immobilization", Biotechnology and Bioengineering 30 (1987), 936–945.

4. Lauren A. Briens, Naoko Ellis, " Hydrodynamics of three-phase fluidized bed systems examined by statistical, fractal, chaos and wavelet analysis methods", Chemical Engineering Science 60 (2005) 6094 – 6106

5. Luo X., Jiang P., Fan L.S. "High-pressure three-phase fluidization: hydrodynamics and heat transfer", A.I.Ch.E. Journal, 43 (1997), 2432–2445.

6. V.K. Bhatia and N. Epstein, "Three-phase fluidization: a generalized wake model ", In: H. Angelino, J.P. Couderc, H. Gibert and H. Lagueric, Editors, "Proceedings of the International Symposium on Fluidization, Its Application", Cepadues-Editions, Toulouse (1974), pp. 380–392

7. Jack T. Cornelissena, Fariborz Taghipoura, Renaud Escudiéa, Naoko Ellis, John R. Gracea, "CFD modelling of a liquid–solid fluidized bed", Chemical Engineering Science 62 (2007) 6334 – 6348.

8. H.M. Jena, G.K. Roy, K.C. Biswal, "Studies on pressure drop and minimum fluidization velocity of gas–solid fluidization of homogeneous well-mixed ternary mixtures in un-promoted and promoted square bed", Chemical Engineering Journal 145 (2008) 16–24

9. Rigby G.R., VanBrokland G.P., Park W.H., Capes C.E. "Properties of bubbles in three-phase fluidized bed as measured by an electro resistivity probe", Chemical Engineering Science 25 (1970), 1729–1741.

10. Lee S.L.P., DeLasa, H.I. "Phase holdups in three-phase fluidized beds." A.I.Ch.E. Journal 33 (1987), 1359–1370.

11. Larachi F., Cassanello M., Chaouki J., Guy C. "Flow structure of the solids in a 3-D gas–liquid–solid fluidized bed." A.I.Ch.E.Journal42 (1996), 2439–2452.

12. Muroyama, K. and L.S. Fan, "Fundamentals of Gas-Liquid-Solid Fluidization", AIChE.J. Vol.3, No.1, (1985), 1-34

13. Fraguío, M.S., Cassanello M.C., Larachi F.,Chaouki,J. "Flow regime transition pointers in three-phase fluidized beds inferred from a solid tracer trajectory", Chemical EngineeringandProcessing45 (2006), 350–358.

14. Dudukovic M.P., Devanathan N., Holub R. "Multiphase reactors Models and experimental verification", Revuedel' Institute Francais du Petrole; 46 (1991),439–465.

15. Kulkarni A.A., Ekambara K., Joshi,J.B., "On the development of flow pattern in a bubble column reactor: experiments and CFD", Chemical Engineering Science; 62 (2007), 1049–1072.

16. Cheung S.C.P., Yeoh G.H., Tu J.Y. "On the numerical study of isothermal vertical bubbly flow using two population balance approaches", Chemical Engineering Science 62 (2007), 4659–4674.

17. Panneerselvam R., Savithri S., SurenderG.D. "CFD based investigations on hydrodynamics and energy dissipation due to solid motion in liquid fluidized bed", Chemical Engineering Journal132 (2007), 159–171.

18. Jiradilok, V.,Gidaspow,D.,Breault,R.W. "Computation of gas and solid dispersion coefficients in turbulent risers and bubbling beds", Chemical Engineering Science62 (2007), 3397–3409.

19. Matonis, D.,Gidaspow,D.,Bahary,M., "CFD simulation of flow and turbulence in a slurry bubble column", A.I.Ch.E.Journal 48 (2007), 1413–1429.

20. Feng W., Wen J., Fan J., Yuan Q., Jia X., Sun Y. "Local hydrodynamics of gas–liquid–nano particles three-phase fluidization", Chemical Engineering Science 60 (2005), 6887–6898.

21. Schallenberg J., En J.H., Hempel D.C. "The important role of local dispersed phase hold-up for the calculation of three-phase bubble columns", Chemical Engineering Science 60 (2005), 6027–6033.

22. S. Ravelli_, A. Perdichizzi, G. Barigozzi. "Description, applications and numerical modelling of bubbling fluidized bed combustion in waste-to-energy plants", Progress in Energy and Combustion Science 34 (2008) 224–253.

23. Shih TH, Liou WW, Shabbir A, Yang Z, Zhu J." A new k–ε eddy viscosity model for high Reynolds number turbulent flows—model development and validation", Comput Fluids 24 (1995), 227–38

24. Srujal Shah, Lappeenranta University of Technology, "Theory and Simulation of Dispersed-Phase Multiphase Flows", 07 May, 2008

25. Kunii D., Levenspiel O., Fluidization Engineering, 2nd Edition, ISBN: 0-409-90233-0, 1991.

26. L. S. Fan, Gas–Liquid–Solid Fluidization Engineering, Butterworth-Heinemann, Boston, 1989

27. Documentation, FLUENT 6.2, 2008.

28. FLUENT user's guide, vols. 1–5. Lebanon, 2001.